CBP ms.23697 Revised – part C

Accumulation of heme oxygenase-1 (HSP32) in *Xenopus laevis* A6 kidney epithelial cells treated with sodium arsenite, cadmium chloride or proteasomal inhibitors

Ena Music, Saad Khan, Imran Khamis, John J. Heikkila

Department of Biology, University of Waterloo, Waterloo, Ontario, Canada

Correspondence:
John J. Heikkila, Ph.D.
Department of Biology
University of Waterloo
Waterloo, ON N2L 3G1, Canada
Phone: 519-885-1211 Ext. 33076; Fax: 519-746-0614
Email: heikkila@uwaterloo.ca

Running Title: Stress-induced HO-1 accumulation in *X. laevis*

Abstract

The present study examined the effect of sodium arsenite, cadmium chloride, heat shock and the proteasomal inhibitors MG132, withaferin A and celastrol on heme oxygenase-1 (HO-1; also known as HSP32) accumulation in *Xenopus laevis* A6 kidney epithelial cells. Immunoblot analysis revealed that HO-1 accumulation was not induced by heat shock but was enhanced by sodium arsenite and cadmium chloride in a dose- and time-dependent fashion. Immunocytochemistry revealed that these metals induced HO-1 accumulation in a granular pattern primarily in the cytoplasm. Additionally, in 20% of the cells arsenite induced the formation of large HO-1-containing perinuclear structures. In cells recovering from sodium arsenite or cadmium chloride treatment, HO-1 accumulation initially increased to a maximum at 12 h followed by a 50% reduction at 48 h. This initial increase in HO-1 levels was likely the result of new synthesis as it was inhibited by cycloheximide. Interestingly, treatment of cells with a mild heat shock enhanced HO-1 accumulation induced by low concentrations of sodium arsenite and cadmium chloride.

Finally, we determined that HO-1 accumulation was induced in A6 cells by the proteasomal inhibitors, MG132, withaferin A and celastrol. An examination of heavy metal and proteasomal inhibitor-induced HO-1 accumulation in amphibians is of importance given the presence of toxic heavy metals in aquatic habitats.

Key Words: heat shock proteins, sodium arsenite, cadmium chloride, amphibian, confocal microscopy, molecular chaperone, frog

Introduction

Sodium arsenite and cadmium chloride are toxic heavy metals that can have deleterious effects on vertebrates ranging from fish and amphibians to man. At the organismal level, sodium arsenite is associated with an increased risk of renal, hepatic and cardiovascular cancers (Del Razo et al., 2001). Cadmium, which accumulates mainly in liver, kidney and reproductive tissues, is labeled a category one human carcinogen due to its implication in various cancers (Waisberg et al., 2003; Bonham et al., 2003; Barbier et al., 2004; Mouchet et al., 2006; Mendez-Armenta and Rios, 2007). Both arsenite and cadmium can be found in ground water originating from natural and anthropogenic sources (Del Razo et al., 2001; Waisberg et al., 2003). At the cellular and molecular level, both arsenite and cadmium toxicity were shown to increase the production of free radicals and reactive oxygen species (ROS) as well as induce metabolic abnormalities, cytoskeletal damage, DNA damage, apoptosis, formation of abnormal proteins and a dysregulation of gene expression (Chou, 1989; Li and Chou, 1992; Liu et al., 2001; Bode and Dong, 2002; Del Razo et al., 2001; Waisberg et al., 2003; Mouchet et al., 2007; Mendez-Armenta and Rios, 2007; Blechinger et al., 2007). Both sodium arsenite and cadmium chloride treatment were also found to inhibit the ubiquitin-proteasome system (UPS), which plays a major role in the degradation of cellular protein through ATP-dependent hydrolysis (Lee and Goldberg, 1998; Kirkpatrick et al., 2003; Awasthani and Wagner, 2005; Yu et al., 2008; Brunt et al., 2012). This system is responsible for the removal of the majority of damaged proteins in the cell.

Previously, it was reported that exposure of mammalian cells to sodium arsenite or cadmium chloride induced the expression of a number of genes that can ameliorate the effects of the heavy metals including those encoding heat shock proteins (HSPs) and heme oxygenase-1 (HO-1, also known as HSP32; Del Razo et al., 2001; Waisberg et al., 2003). HSPs are classified as molecular chaperones since they are involved in the folding and translocation of cellular proteins (Morimoto,

1998; Katschinski, 2004; Morimoto, 2008). They are grouped into at least six families based on size including HSP110, HSP90, HSP70, HSP60, HSP40, and the small HSPs (sHSPs). HSPs are generally highly conserved, and have been found in organisms ranging from bacteria to humans. Under stressful conditions, stress-inducible HSPs prevent the aggregation of unfolded proteins. Additionally, they contribute to protein refolding once the stress is alleviated and are involved in the degradation of proteins damaged beyond repair. Stress-induced accumulation of HSPs is primarily mediated by the *trans*-acting regulatory factor, heat shock factor 1 (HSF1), and the *cis*-acting heat shock element (HSE) located in the promoter region of *hsp* genes.

HO-1, which is involved in heme metabolism, also plays a role in the protection of cells against oxidative stress, likely through the effects of its catalytic by-products (Takeda et al., 1995; Gozzelino et al., 2010; Correa-Costa et al., 2012). For example, bilirubin is a potent antioxidant since it can scavenge ROS (Morita et al., 1997). Furthermore, HO-1 was detected at high levels in prostate and brain tumours, where it appears to have a cytoprotective effect (Maines and Abrahamsson, 1996; Hara et al., 1996; Fang et al., 2004). It was suggested that inhibition of HO-1 may be beneficial in treating cancer as HO-1 catalytic by-products were found to have an anti-apoptotic and angiogenic effect, contributing to the vascularisation of tumours (Brouard et al., 2000; Deshane et al., 2007). Also, induction of HO-1 has been associated with neurological disorders such as Alzheimer's, Huntington's, and Parkinson's disease (Smith et al., 1994; Schipper et al., 1998; Pappolla et al., 1998). Sodium arsenite and cadmium chloride have each been shown to induce the accumulation of HO-1 in mammalian cells (Masuya et al., 1998; Fauconneau et al., 2002; Lee et al., 2005; Miyamoto et al., 2009; Teng et al., 2013). It was suggested that these metals induce oxidative damage that results in the enhanced expression of the *ho-1* gene mediated through the Maf recognition elements (MARE) / nuclear factor-erythroid 2 family member (Nrf2) and p38 mitogen-activated protein kinase (p38 MAPK) pathways (Elbirt et al., 1998; Alam et al., 2000; Lau et al., 2012). Additionally, cadmium chloride-induced *ho-1* gene expression may involve the cadmium response element (CdRE), as well as the transcription factors HSF1 and pescadillo (Sikorski et al., 2006; Koizumi et al., 2007).

Amphibians, given their aquatic habitat, are sensitive to the presence of sodium arsenite or cadmium chloride in their environment. For example, in the South African clawed frog, *Xenopus laevis*, sodium arsenite induced malformations during embryogenesis and metamorphosis and caused alterations in F-actin cytoskeletal structure in cultured cells (Gornati et al., 2000; Gellalchew and Heikkila, 2005; Davey et al., 2008). Also, cadmium was determined to have toxic and genotoxic effects during *Xenopus* development that included ocular anomalies, bent notochord and

heart kidney, ovary and gut dysplasia and altered thyroid activity (Plowman et al., 1994; Mouchet et al., 2006; Sharma and Patino, 2008). Finally, both sodium arsenite and cadmium chloride induced the accumulation of *Xenopus* HSPs, including the small HSP family HSP30, as well as the inhibition of proteasome activity as indicated by an increase in the level of ubiquitinated protein and a decrease in chymotrypsin-like activity (Gordon et al., 1997; Lang et al., 2000; Gornati et al., 2002; Heikkila, 2004; Gellalchew and Heikkila, 2005; Voyer and Heikkila, 2008; Woolfson and Heikkila, 2009; Young et al., 2009; Heikkila, 2010; Brunt et al., 2012). In contrast to HSPs, there is no available data, to the best of our knowledge, on the effects of sodium arsenite or cadmium chloride on HO-1 accumulation in amphibian model systems. In fact, information regarding the expression of the *ho-1* gene is limited to a single report examining its constitutive expression during early embryogenesis of *Xenopus laevis* (Shi et al., 2008).

In the present study, we examined the effect of heat shock, sodium arsenite and cadmium chloride treatment of *Xenopus laevis* A6 kidney epithelial cells on HO-1 accumulation and localization by immunoblot and immunocytochemical analysis, respectively. The levels of HO-1 were compared to HSP30, which was previously shown by our laboratory to be induced by all of the stressors in this study. Furthermore, we investigated the effect of a mild heat shock in conjunction with sodium arsenite or cadmium chloride exposure. Given the previous finding that these metals can inhibit proteasomal activity in A6 cells (Brunt et al., 2012), we examined the effect of the proteasomal inhibitors MG132, withaferin A and celastrol on HO-1 accumulation and localization.

2. Materials and Methods

2.1. Maintenance and treatment of Xenopus laevis A6 kidney epithelial cells

X. laevis A6 kidney epithelial cells were obtained from the American Type Culture Collection (CCL-102; Rockville, MD, USA). Cells were cultured in 70% Leibovitz (L)-15 media (Sigma-Aldrich, Oakville, ON, Canada) and supplemented with 10% fetal bovine serum, 100 units/mL penicillin and 100 μg/mL streptomycin (all from Sigma-Aldrich) at 22 °C in T75 cm^2 BD Falcon tissue culture flasks (VWR International, Mississauga, ON). Flasks containing cells that had achieved a confluency of 80-90% were used for experiments. Cells were maintained at 22 °C or subjected to heat shock at 30, 33 or 35 °C for 2 h followed by a 2 h recovery at 22 °C. Additionally, cells were incubated with 5 to 50 μM sodium arsenite, 10 to 200 μM cadmium chloride, 5 to 30 μM MG132 (carbobenzoxy–L-leucyl–L-leucyl–L-leucinal; dissolved in dimethylsulphoxide (DMSO; both from Sigma-Aldrich; Young and Heikkila, 2010), 1 to 10 μM withaferin A (dissolved in

DMSO; Enzo Life Sciences, Plymouth Meeting, PA; Khan et al., 2012) or 1 to 7.5 μM celastrol (dissolved in DMSO; Cayman Chemical, Ann Arbor, MI, USA; Walcott and Heikkila, 2010) at 22 °C. In time course experiments, cells were treated with 30 μM sodium arsenite, 100 μM cadmium chloride, 30 μM MG132, 5 μM withaferin A or 2.5 μM celastrol at 22 °C for periods of time ranging from 0 to 48 h. In recovery experiments, cells were treated with sodium arsenite for 24 h followed by removal of media, rinsing of the flasks with media and incubation in fresh media for 0 to 48 h. Some cells recovering from sodium arsenite treatment were also incubated with 100 μM cycloheximide (CHX; dissolved in water; Sigma-Aldrich) for the duration of the recovery period at 22 °C. In experiments that combined a mild heat shock with chemical treatment, sodium arsenite, cadmium chloride were added to flasks of cells at the indicated concentrations and then incubated in a heated water bath at 30 °C for 12 h. Following treatment, media was removed, and cells were rinsed with 2 mL of 65% Hank's balanced salt solution (HBSS; Sigma-Aldrich) followed by the addition of 1 mL 100% HBSS. Cells were detached from the flask by scraping and then transferred to a 1.5 mL microcentrifuge tube. Cells were pelleted by means of centrifugation for 1 min at 21,920 *g*. The pelleted cells were stored at -80 °C prior to protein isolation.

2.2. Protein isolation and immunoblot analysis

The isolation of protein from A6 cells was performed as previously described (Young et al., 2009). Protein quantification was performed utilizing the bicinchoninic acid (BCA) method following the manufacturer's protocol (Pierce, Rockford, IL, USA). Protein separation employing SDS-PAGE and transfer of proteins to nitrocellulose membrane was performed as previously described (Young et al., 2009; Khamis and Heikkila, 2013). The membranes were incubated with rabbit anti-HO-1 antibody (1:500, Enzo Life Sciences, Farmingdale, NY), rabbit anti-*Xenopus* HSP30 antibody (1:1000; Fernando and Heikkila, 2000), or rabbit anti-actin polyclonal antibody (1:200, Sigma-Aldrich). The nitrocellulose membranes were then incubated with alkaline phosphatase-conjugated goat anti-rabbit (BioRad, 1:3000 dilution). For detection, the membrane was incubated in alkaline phosphatase buffer (100 mM Tris base, 100 mM NaCl, 50 mM $MgCl_2$ (pH 9.5)), 0.3% 4-nitro blue tetrazolium (NBT; Roche Diagnostics, Mississauga, ON, Canada), and 0.17% 5-bromo-4-chloro-3-indolyl phosphate, toluidine salt (BCIP; Roche Diagnostics) until the bands were visible. Image J software (Version 1.46) was used to perform densitometric analysis within the range of linearity on all blots, with experiments performed at least in triplicate. The average values obtained were graphed as a percentage of the maximum value of either HO-1 or HSP30 bands. Vertical error bars display the standard error of the mean. Statistical analysis was performed on normalized data using

a one-way analysis of variance (ANOVA) with a Tukey's post-test ($p<0.05$; indicated by *) to determine if statistically significant differences existed between samples.

2.3. Immunocytochemistry and laser scanning confocal microscopy (LSCM)

Immunofluorescence analyses were performed as detailed previously (Young et al., 2009; Khan et al., 2012). A6 cells were cultured on glass coverslips in sterile petri dishes at 22 °C for 24 h. The cells were then incubated at 33 °C for 2 h followed by a 2 h recovery at 22 °C or incubated with either 10 μM sodium arsenite, 100 μM cadmium chloride, 20 μM MG132, 2.5 μM celastrol, or 5 μM withaferin A at 22 °C for 24 h. After treatment, L-15 media was removed and the cells were washed twice in phosphate-buffered saline (PBS; 1.37 M NaCl, 67 mM Na_2HPO_4, 26 mM KCl, 14.7 mM H_2PO_4, 1 mM $CaCl_2$, 0.5 mM $MgCl_2$, pH 7.4) and the coverslips were transferred to new small petri dishes. Fixation of the cells was carried out with 3.7% paraformaldehyde in PBS (BDH Inc., Toronto, ON, Canada) for 15 min. Cells were rinsed 3 times for 5 min with PBS and then permeabilized with 0.3% Triton X-100 (Sigma-Aldrich) in PBS for 10 min followed by three washes with PBS. A6 cells were incubated with 3.7% (w/v) filtered bovine serum albumin (BSA) fraction V in PBS (Fisher Scientific, Ottawa, ON, Canada) for 1 h. Cells were then incubated with either affinity-purified rabbit anti-*Xenopus* HSP30 (1:500) or anti-HO-1 (1:200) antibody in 3.7% BSA for 1 h. Cells were washed 3 times with PBS for 2 min each. Indirect labeling was carried out in the dark for 30 min with fluorescent-conjugated goat anti-rabbit Alexa Fluor 488 (Molecular Probes, Eugene, OR, USA) in BSA at a 1:2000 dilution. After washing 3 times with PBS for 3 min each, cells were incubated with rhodamine-tetramethylrhodamine-5-isothiocyanate phalloidin (TRITC; 1:100; Molecular Probes) for 15 min to visualize the actin cytoskeleton. After washing 3 times with PBS, coverslips were dried and mounted on a microscope slide with Vectashield mounting medium (Vector Laboratories Inc., Burlingame, CA), which contained 4,6-diamidino-2-phenylindole (DAPI; Vector Laboratories Inc.) for the staining of nuclei. The slides were blotted dry and clear nail polish was used as an adhesive to bind coverslips to glass microscope slides. Slides were stored at 4 °C for a minimum of 1 h or until required. Cells were visualized using a Zeiss Axiovert 200 confocal microscope with Zen 2009 software (Carl Zeiss Canada Ltd., Mississauga, ON, Canada). Images were viewed with Zen 2009 Light Edition software.

Results

3.1. Characterization of heme oxygenase-1 (HO-1) protein in Xenopus laevis

The *X. laevis* putative HO-1 amino acid (aa) sequence was derived from the nucleotide sequence of a HO-1 cDNA originally isolated from an oocyte cDNA library (Figure 1). *X. laevis* HO-1 is 291 aa in length with an estimated size of 33.5 kDa and includes 8 heme binding pocket residues and a heme ligand binding site at H28. A comparison of the percent identity of the *X. laevis* HO-1 aa sequence with HO-1 aa sequences from other selected organisms and the constitutive HO-2 from *X. laevis* is shown in Table 1. *X. laevis* HO-1 shares 91% identity with *X. tropicalis* HO-1 while the percent identity with other organisms including chicken, duck, human, mouse, alligator and zebrafish HO-1 ranged from 63 to 45%. However, when percent identity was determined for a particularly conserved region (P129-R186) of *X. laevis* HO-1, the percent identity ranged from 100% identity with *X. tropicalis* HO-1 to 69% with zebrafish HO-1. This region contains 4 of the 8 heme binding pocket residues and is indicated in Figure 1 with a dashed line. *X. laevis* constitutive HO-2 shared only 53% identity with HO-1 and 74% in the HO-1 conserved region. Since an anti-*X. laevis* HO-1 antibody was not available for immunoblot and immunocytochemical analysis, we utilized an antibody (Enzo Life Sciences, BML-HC3001) that was made against a synthetic peptide (DLSEALKEATKEVH) derived from a human HO-1 conserved sequence, which shared 100% identity with *X. laevis* HO-1 (Figure 1). Previous studies employed this anti-HO-1 antibody to study stress-induced HO-1 accumulation in human cells (Hock et al., 2004; Hanneken et al., 2006).

3.2. Heme oxygenase-1 (HO-1) is not induced by heat shock

Initially, the effect of heat shock on HO-1 accumulation in A6 cells was examined by immunoblot analysis. As shown in Figure 2, A6 cells exposed to 30, 33 or 35 °C for 2 h followed by a 2 h recovery period at 22 °C did not induce detectable HO-1 accumulation even after longer incubation times as shown in Figure 8A. In contrast, HSP30 accumulation was induced at all 3 temperatures, which is in agreement with our previous findings (Gellalchew and Heikkila, 2005). In these experiments, sodium arsenite, which enhanced the levels of both HO-1 and HSP30, was employed as a positive control since previous studies demonstrated that HO-1 accumulation was induced by sodium arsenite in murine, and human cells (Fauconneau et al., 2002; Gong et al., 2002).

3.3. HO-1 accumulation is induced by sodium arsenite and cadmium chloride in a concentration- and time-dependent manner

An examination of the effect of different concentrations of sodium arsenite for 24 h on HO-1 accumulation in A6 cells revealed that HO-1 was detectable at 5 μM, peaked at 10 μM and then declined to lower levels at higher concentrations (Fig. 3A). Compared to maximum levels of HO-1

found with 10 μM sodium arsenite treatment, the levels of HO-1 accumulation at 5 μM was 79% while at 50 μM the level was reduced to 56% (Fig. 3B). HSP30 accumulation in A6 cells was first detected using 10 μM sodium arsenite with peak levels at 20 to 30 μM and a slight reduction at 50 μM. In a comparable analysis with cadmium chloride, both HO-1 and HSP30 accumulation was detected in cells treated with 50 μM cadmium chloride, peaked at 100 μM and then declined to lower levels at 200 μM (Fig. 3C). Densitometric analysis determined that in comparison to cells treated with 100 μM cadmium chloride, the level of HO-1 accumulation at 50 and 200 μM were 81 and 32% of maximal values, respectively, whereas HSP30 values at the same concentrations were 54 and 73%, respectively (Fig. 3D).

In time course studies with A6 cells subjected to 30 μM sodium arsenite, HO-1 and HSP30 accumulation were first detectable at 8 h and then increased in a time-dependent manner until the final time point of 48 h (Fig. 4A). Densitometric analysis determined that at 8, 12, and 24 h, HO-1 signal intensities were approximately 12, 30, and 85% of maximum, respectively (Fig. 4B). A similar temporal pattern was observed for HSP30. In cells treated with 100 μM cadmium chloride for 4 to 48 h, minimal levels of HO-1 and HSP30 accumulation were first detected at 8 h followed by a time-dependent increase up to 48 h (Fig. 4C). Densitometry indicated that the values of HO-1 accumulation at 8, 12, and 24 h were 7, 44 and 49%, respectively, compared to the maximum value at 48 h (Fig. 4D). A similar phenomenon was noted with HSP30, except that a near maximal value of 92% was detected after 24 h of cadmium chloride treatment.

The induction of HO-1 in A6 cells by sodium arsenite or cadmium chloride appears to involve *de novo* transcription and translation. For example, treatment of cells with the transcriptional inhibitor, actinomycin D, prior to sodium arsenite or cadmium chloride treatment inhibited the accumulation of HO-1 and HSP30 (Fig. 5A). Cycloheximide, an inhibitor of protein synthesis, likewise prevented sodium arsenite- and cadmium chloride-induced HO-1 and HSP30 accumulation (Fig. 5B).

3.4. Cellular localization of sodium arsenite- and cadmium chloride-induced HO-1

Immunocytochemistry was used to examine the effect of heat shock, sodium arsenite, and cadmium chloride on HO-1 localization in A6 cells. HO-1 was not detected under heat shock conditions (Fig. 6) in contrast to HSP30, which was detected in approximately 85-100% of cells (data not shown). Approximately 80% of cells treated with 10 μM sodium arsenite for 24 h exhibited HO-1 accumulation in a punctate pattern with enrichment in the perinuclear region of the cytoplasm. Interestingly, 20% of the sodium arsenite-treated cells displayed HO-1 accumulation in large perinuclear structures (white arrows). Similar to arsenite, cadmium chloride induced HO-1

accumulation in a granular pattern that was detected in approximately 80% of cells. In essentially all of the sodium arsenite- and cadmium chloride-treated cells, control-like actin stress fibers and an intact F-actin cytoskeleton were observed. However, a minor amount of membrane ruffling was noted in some cells subjected to each of the stressors.

3.5. Examination of HO-1 accumulation in cells recovering from sodium arsenite

The next phase of this study examined the levels of HO-1 accumulation during recovery of cells from 30 μM sodium arsenite for 24 h (Fig. 7A). The levels of HO-1 increased during recovery up to 12 h followed by a decrease at 24 h and a 4-fold reduction at 48 h. Similar results were observed for the levels of HSP30, with an increase in accumulation from 0 to 12 h recovery, followed by a decrease in HSP30 accumulation after 24 h of recovery, and a 2-fold reduction after 48 h of recovery compared to maximal values. In order to monitor the decay pattern of HO-1 during recovery from sodium arsenite in the absence of translation, cycloheximide (CHX) was employed. As shown in Figure 7B, preincubation of cells with 100 μM CHX for 6 h completely inhibited the sodium arsenite-induced transient increase in accumulation of both HO-1 and HSP30 after 12 h of recovery such that the levels of these proteins decreased gradually over 48 h. These results show that the transient increase in HO-1 and HSP30 levels after incubation with sodium arsenite is due to new synthesis since inhibition of protein synthesis prevented this response. Similar results were obtained with A6 cells recovering from a 12 h treatment with 100 μM cadmium chloride treatment (data not shown).

3.6. Mild heat shock enhanced sodium arsenite- and cadmium chloride-induced HO-1 accumulation

Previous studies in our laboratory determined that elevated temperatures enhanced sodium arsenite- or cadmium chloride-induced HSP30 accumulation (Woolfson and Heikkila, 2009; Young et al., 2009). Given these results we examined the effect of a mild heat shock on sodium arsenite- or cadmium chloride-induced upregulation of HO-1 levels in A6 cells. Treatment of cells with a mild heat shock of 30 °C for 12 h did not result in detectable levels of HO-1 or HSP30 (Fig. 8A). Furthermore, exposure of cells to 10 μM cadmium chloride for 12 h at 22 °C did not induce detectable levels of HO-1 or HSP30 although cadmium treatment at 30 °C did induce a slight increase in HO-1 levels to 3% of peak levels (Fig. 8B). Treatment of A6 cells with 10 μM sodium arsenite alone resulted in enhanced levels of HO-1 and HSP30 to 9% and 30%, respectively, of maximum levels. Compared to 10 μM sodium arsenite alone, the highest levels of HO-1 (3-fold) and HSP30 (11-fold) accumulation occurred in cells subjected to a mild heat shock plus sodium

arsenite. When cells were treated with sodium arsenite and cadmium chloride simultaneously at 22 °C, HO-1 and HSP30 accumulation were 56% and 16% of the maximum values, respectively.

3.7. Proteasomal inhibitors induced HO-1 accumulation in a concentration- and time-dependent manner

Given our previous finding that sodium arsenite and cadmium chloride inhibited proteasomal activity and induced *hsp30* gene expression (Brunt et al., 2012), we examined the effect of MG132, a well-characterized proteasomal inhibitor, on HO-1 accumulation in A6 cells. As shown in Figure 9A, cells treated with MG132 displayed detectable levels of HO-1 accumulation at 5 μM, peaked at 20 μM and reduced levels at 30 μM (Fig. 9A). Densitometric analysis indicated that HO-1 accumulation at 5 μM MG132 was 33% of the maximal density, while 10 and 30 μM were 65 and 53%, respectively (Fig. 9B). Accumulation of HSP30 induced by 5 μM MG132 was 59% of the maximum value, while the densities for 10 and 30 μM MG132 treatments were 87 and 68%, respectively. In time course studies employing 30 μM MG132, minimal HO-1 and HSP30 accumulation was detected at 8 h followed by increased levels in a time-dependent manner up to 48 h (Fig. 9C). Densitometric analysis determined that the levels of HO-1 accumulation at 8, 12, and 24 h were 29, 66 and 87%, respectively, of the maximum density while for HSP30 the same time points exhibited densities of 16, 45, 76%, respectively, compared to peak values (Fig. 9D). As found with sodium arsenite and cadmium chloride, actinomycin D and cycloheximide pretreatment each inhibited HO-1 and HSP30 accumulation suggesting the involvement of *de novo* transcription and translation in their induction (data not shown). Finally, treatment of cells with a mild heat shock of 30 °C significantly enhanced MG132-induced accumulation of both HO-1 and HSP30 compared to cells treated at 22 °C (data not shown).

Two other proteasomal inhibitors, withaferin A and celastrol, that were shown to induce HSP30 accumulation (Walcott and Heikkila, 2010; Khan et al., 2012), also enhanced HO-1 accumulation in A6 cells. In preliminary dose-response experiments, maximal accumulation of HO-1 occurred with 5 μM withaferin A and 2.5 μM celastrol (data not shown). In time course studies, HO-1 accumulation was initially detected in cells treated with 5 μM withaferin A for 8 h with maximum levels at 16 h and a slight reduction at 24 h (Fig. 10A, B). In contrast to HO-1, maximum levels of HSP30 were found at 24 h. Additionally, celastrol-induced HO-1 and HSP30 accumulation occurred initially in cells treated with 2.5 μM celastrol for 8 h and maximal levels were observed in cells treated for 24 h (Fig. 10C). A 20-fold increase in HO-1 accumulation was observed in cells

treated for 16 h in comparison to 8 h. This was greater than the 4-fold increase observed with HSP30 during the same time period (Fig. 10D).

3.8 Localization of HO-1 accumulation in response to selected proteasomal inhibitors

Finally, immunocytochemistry was employed to examine the effect of MG132, withaferin A, and celastrol on HO-1 localization in A6 cells (Fig. 10). HO-1 was detected in a punctate pattern in approximately 65% of MG132-treated cells, while withaferin A and celastrol induced HO-1 accumulation in 90 and 85% of cells, respectively. Proteasomal inhibitor-treated A6 cells generally displayed an intact F-actin cytoskeleton. However, in some cells treated with celastrol, we observed a rounded cell shape and disrupted actin cytoskeleton as indicated by F-actin localization to the cell periphery. It is possible that celastrol might inhibit nuclear factor kappaB (NF-κB), which is linked to decreased levels of cell adhesion molecules that are required for proper attachment of the cytoskeleton to the extracellular matrix (Collins et al., 1995; Tozawa et al., 1995).

Discussion

The present study has demonstrated that treatment of amphibian cells with heavy metals and proteasomal inhibitors but not heat shock induced the accumulation of HO-1. These findings are of significance given the contamination of numerous aquatic habitats with heavy metals and other toxins. Initial immunoblot and immunocytochemical studies determined that HO-1 accumulation in *X. laevis* A6 kidney epithelial cells was not induced by heat shock in contrast to HSP30. A lack of heat-inducibility with respect to HO-1 accumulation was reported in a variety of mammalian cell lines, including human alveolar macrophage, hepatoma, glioma, HeLa, fibroblast, erythroblast, and HL60 leukemia (Yoshida et al., 1988; Keyse and Tyrrell, 1989; Taketani et al., 1989; Mitani et al., 1990; Okinaga et al., 1996). However, other studies reported that heat shock enhanced HO-1 accumulation in rat liver, kidney, heart and brain as well as in murine Sertoli cells, human fibroblasts, and in rat and human hepatoma cell lines (Taketani et al., 1988; Keyse and Tyrrell, 1989; Mitani et al., 1990; Raju and Maines, 1994; Lee et al., 1996; Bechtold and Brown, 2003). The mechanism(s) responsible for the differences in the heat inducibility of HO-1 accumulation in different cell types or tissues is not known. However, previous studies with a human erythroid cell line revealed that a HSE found in the regulatory region of the *ho-1* gene was repressed, possibly by transcription factors that interacted with a downstream purine-rich region (Okinaga et al., 2006). While it is possible that this mechanism may account for the lack of heat shock inducibliity of HO-1

accumulation in A6 cells, unfortunately the regulatory regions of the *X.s laevis ho-1* gene have not been isolated and sequenced.

Treatment of *Xenopus* A6 cells with the heavy metals sodium arsenite and cadmium chloride resulted in HO-1 accumulation in a dose- and time-dependent manner. Furthermore, heavy metal-induced HO-1 accumulation was inhibited by actinomycin D, a transcriptional inhibitor, and by the translational inhibitor cycloheximide. Sodium arsenite was also found to induce HO-1 accumulation in chicken hepatoma cells as well as in the human cell lines, HeLa and HL60 leukemia (Taketani et al., 1989; Elbirt et al., 1998; Ryter et al., 2006). Furthermore, cadmium chloride-induced HO-1 accumulation was documented in fish and mammalian systems (Taketani et al., 1989; Alam et al., 2000; Ryter et al., 2006; Søfteland et al., 2010; Williams and Gallagher, 2013). Previous studies with mammalian cells reported that transcriptional activation of the *ho-1* gene in response to oxidative damage to cellular protein induced by sodium arsenite or cadmium chloride treatment involved the Nrf2 pathway including the transcriptional repressor Bach1 (Alam et al., 2000; Suzuki et al., 2003; Waisberg et al., 2003; Galazyn-Sidorczuk et al., 2009). It was determined that treatment of cells with sodium arsenite inactivated Bach1 while cadmium chloride induced its export from the nucleus (Del Razo et al., 2001; Suzuki et al., 2003; Samuel et al., 2005; Reichard et al., 2008). In each situation the lack of a functional repressor resulted in the Nrf2-mediated activation of the *ho-1* gene expression. Another possibility for the upregulation of *ho-1* gene expression by cadmium chloride involves the binding of transcription factors to the *cis*-acting cadmium-responsive element (CdRE) found in the 5' regulatory region (Takeda et al., 1995). In human renal epithelial cells the transcription factor pescadillo interacted specifically with the CdRE (Sikorski et al., 2006). Also, pescadillo overexpression increased the transcriptional activity of the human *ho-1* gene promoter. Furthermore, it was suggested that in cadmium chloride-treated HeLa cells, HSF1 may interact with pescadillo bound to CdRE or with other transcription factors bound to adjacent regulatory elements resulting in an enhanced expression of the *ho-1* gene (Koizumi et al., 2007). Finally, a study with mouse hepatoma cells suggested that cadmium-induced *ho-1* gene expression might occur through stabilization of Nrf2 protein (Stewart et al., 2003). Hopefully, future studies will determine whether these possible mechanism(s) for sodium arsenite- or cadmium chloride-induced *ho-1* gene activation extend to *Xenopus*.

The present study has shown that proteasomal inhibitors including MG132, withaferin A and celastrol induced HO-1 accumulation in A6 cells. While MG132-induced accumulation of HO-1 was documented in mammalian cells, enhanced levels of HO-1 were induced by lower concentrations and at shorter time points than found with *Xenopus* A6 cells. For example, HO-1

was detectable in A6 cells after a 5 μM MG132 treatment for 24 h with higher levels from 10 to 30 μM. In contrast, mouse astrocytes displayed elevated levels of HO-1 with only 1 μM MG132 after 2 h (Chen and Regan, 2005; Cui et al., 2013). In the present study, two anti-inflammatory plant products, withaferin A and celastrol, which were previously shown to inhibit proteasomal activity and induce HSP30 in *Xenopus* A6 cells (Walcott and Heikkila, 2010; Khan et al., 2012), also induced HO-1 accumulation. In mammalian studies, withaferin A increased HO-1 accumulation in human choroidal endothelial cells while celastrol treatment induced *ho-1* gene expression in rat vascular smooth muscle cells and cerebral cortical cultures and in a human keratinocyte cell line (Bargagna-Mohan et al., 2006; Yu et al., 2010; Seo et al., 2011; Chow et al., 2013). While the mechanism for proteasomal inhibitor induced accumulation of HO-1 in *Xenopus* cells is not known, a number of studies with mammalian cells proposed that proteasomal inhibitor-induced accumulation of HO-1 involves the transcription factor, Nrf2 (Wu et al., 2004; Yamamoto et al., 2010). Previously, Wu et al. (2004) reported that MG132-induced accumulation of HO-1 in murine macrophages occurred through the activation of the p38-MAPK pathway. Subsequently, Kastle et al. (2012) determined that proteasomal inhibition induced the deacetylation of HDAC6 resulting in the subsequent phosphorylation of p38-MAPK and activation of the Nrf2 pathway. Finally, it was suggested that proteasomal inhibitors might enhance the stability of Nrf2 and prolong its activity by preventing its on-going degradation (Stewart et al., 2003; Martin et al., 2004).

Immunocytochemical analysis of A6 cells confirmed the presence of HO-1 accumulation in response to sodium arsenite, cadmium chloride, MG132, withaferin A or celastrol treatment primarily in the perinuclear region in a punctate pattern. These results were expected since HO-1 is primarily an ER protein that is anchored to the endoplasmic reticulum by a single C-terminal transmembrane region (Ryter et al., 2006; Gottlieb et al., 2012). Interestingly, large HO-1 antibody-staining structures were detected in about 20% of cells treated with sodium arsenite treatment. In a recent study, it was determined that NADPH cytochrome P450 reductase can promote oligomerization of HO-1 into higher ordered complexes also containing biliverdin reductase (Huber et al., 2009; Linnenbaum et al., 2012). It is possible that a similar phenomenon may occur with HO-1 in A6 cells.

Finally, the present study determined that incubation of A6 cells with low concentrations (10 μM) of sodium arsenite or cadmium chloride plus a concurrent mild heat shock (30 °C) enhanced the levels of HO-1 accumulation compared to the different stressors individually. Previously, it was reported that cellular uptake of both sodium arsenite and cadmium chloride increased with elevated temperatures in mammals and fish (McGeachy and Dixon, 1989; Souza et al., 1997; Saydam et al.,

2003). Thus, it is possible that the mild heat shock may enhance the uptake of sodium arsenite, cadmium chloride or MG132 into A6 cells which may in turn increase their ability to activate the Nrf2 pathway thereby activating *ho-1* gene expression as previously discussed. It is also tenable that the mild heat shock may have increased the amount of oxidative stress in A6 cells, which could further activate the Nrf2 pathway.

In summary, the present study found that *Xenopus* HO-1 accumulation was induced by sodium arsenite, cadmium chloride and proteasomal inhibitors but not heat shock. Additional basic information regarding stress-induced HO-1 accumulation is of importance given that it has been implicated in a variety of diseases and conditions that are associated with oxidative stress or proteasomal inhibition, including Alzheimer's disease, diabetes, atherosclerosis, and myocardial infarction (Takahashi et al., 2000; Juan et al., 2001; Turkseven et al., 2005; Liu et al., 2005). Additionally, aquatic organisms, including amphibians, are quite susceptible to the deleterious effects of toxicants such as sodium arsenite and cadmium chloride. Thus, HO-1 may be of value as a biomarker for studies involving environmental contamination by cadmium chloride, sodium arsenite or other agents. The present study has also shown that HO-1 accumulation by these metals was enhanced by mild heat shock. This last finding is of importance given the global rise in temperature over the last number of decades and its potential effect on aquatic organisms, especially those in contaminated lakes or rivers.

Acknowledgements. This research was supported by a Natural Sciences and Engineering Research Council (NSERC) grant to JJH. JJH is the recipient of a Canada Research Chair in Stress Protein Gene Research while SK is the recipient of an NSERC postgraduate scholarship.

References

Alam, J., Wicks, C., Stewart, D., Gong, P., Touchard, C., Otterbein, S., Choi, A.M.K., Burow, M.E., Tou, J. 2000. Mechanism of heme oxygenase-1 gene activation by cadmium in MCF-7 mammary epithelial cells: role of p38 kinase and Nrf2 transcription factor. J. Biol. Chem. 275, 27694-27702.

Awasthi, N., Wagner, B.J. 2005. Upregulation of heat shock protein expression by proteasome inhibition: an antiapoptotic mechanism in the lens. Invest. Ophthalmol. Vis. Sci. 46, 2082-2091.

Barbier, O., Jacquillet, G., Tauc, M., Poujeol, P., Cougnon, M. 2004. Acute study of interaction among cadmium, calcium, and zinc transport along the rat nephron in vivo. Am. J. Physiol. Renal. Physiol. 287, 1067-1075.

Bargagna-Mohan, P., Ravindranath, P.P., Mohan, R. 2006. Small molecule anti-angiogenic probes of the

ubiquitin proteasome pathway: Potential application to choroidal neovascularization. Invest. Ophthalmol. Vis. Sci. 47, 4138-4145.

Bechtold, D.A., Brown, I.R. 2003. Induction of Hsp27 and Hsp32 stress proteins and vimentin in glial cells of the rat hippocampus following hyperthermia. Neurochem. Res. 28, 1163-1174.

Blechinger, S.R., Kusch, R.C., Haugo, K., Matz, C., Chivers, D.P., Krone, P.H. 2007. Brief embryonic cadmium exposure induces a stress response and cell death in the developing olfactory system followed by long-term olfactory deficits in juvenile zebrafish. Toxicol. Appl. Pharamacol. 224, 72-80.

Bode, A.M., Dong, Z. 2002. The paradox of arsenic: molecular mechanisms of cell transformation and chemotherapeutic effects. Crit. Rev. Oncol. Hematol. 42, 5-24.

Bonham, R.T, Fine, M.R., Pollock, F.M., Shelden, E.A. 2003. Hsp27, Hsp70, metallothionein in MDCK and LLC-PK1 renal epithelial cells: effects of prolonged exposure to cadmium. Toxicol. Appl. Pharmacol. 191, 63-73.

Brouard, S., Otterbein, L.E., Anrather, J., Tobiasch, E., Bach, F.H., Choi, A.M., Soares, M.P. 2000. Carbon monoxide generated by heme oxygenase 1 suppresses endothelial cell apoptosis. J. Exp. Med. 192, 1015-1026.

Brunt, J., Khan, S., Heikkila, J.J. 2012. Sodium arsenite and cadmium chloride induction of proteasomal inhibition and HSP accumulation in *Xenopus laevis* A6 kidney epithelial cells. Comp. Biochem. Physiol. C. Toxicol. Pharmacol. 55, 307-317.

Chen J., Regan R.F. 2005. Increasing expression of heme oxygenase-1 by proteasome inhibition protects astrocytes from heme-mediated injury. Curr. Neurovasc. Res. 2, 189-196.

Chou, I.N. 1989. Distinct cytoskeletal injuries induced by As, Cd, Co, Cr and Ni compounds. Biomed. Environ. Sci. 2, 358-365.

Chow, A.M., Tang, D.W., Hanif, A., Brown, I.R. 2013. Induction of heat shock proteins in cerebral cortical cultures by celastrol. 18, 155-160.

Collins, T., Read, M.A., Neish, A.S., Whitley, M.Z., Thanos, D., Maniatis, T., 1995. Transcriptional regulation of endothelial cell adhesion molecules: NF-kappa B and cytokine-inducible enhancers. FASEB J. 9, 899–909.

Correa-Costa, M., Amano, M.T., Camara, N.O. 2012. Cytoprotection behind heme oxygenase in renal diseases. World J. Nephrol. 1, 4-11.

Cui, W., Bai, Y., Luo, P., Miao, L., Cai, L. 2013. Preventive and therapeutic effects of MG132 by activating Nrf2-ARE signalling pathway on oxidative stress-induced cardiovascular and renal injury. Oxid. Med. Cell Longev. doi: 10.1155/2013/306073.

Davey, J.C., Nomikos, A.P., Wungjiranirun, M., Sherman, J.R., Ingram, L., Batki, C., Lariviere, J.P., Hamilton, J.W. 2008. Arsenic as an endocrine disruptor: Arsenic disrupts retinoic acid receptor and thyroid hormone receptor-mediated gene regulation and thyroid hormone-mediated amphibian tail metamorphosis. Environ. Health Perspect. 116, 165-172.

Del Razo, L.M., Quintanilla-Vega, B., Brambila-Colombres, E., Calderon-Aranda, E.S., Manno M., Albores, A. 2001. Stress proteins induced by arsenic. Toxicol. Appl. Pharmacol. 177, 132-148.

Deshane, J., Chen, S., Caballero, S., Grochot-Przeczek, A., Was, H., Li Calzi, S., Lach, R., Hock, T.D., Chen, B., Hill-Kapturczak, N., Siegal, G.P., Dulak, J., Jozkowicz, A., Grant, M.B., Agarwal, A. 2007. Stromal cell-derived factor 1 promotes angiogenesis via a heme oxygenase 1-dependent mechanism. J. Exp. Med. 204, 605-618.

Elbirt K.K., Whitmarsh A.J., Davis R.J., Bonkovsky H.L. 1998. Mechanism of sodium arsenite mediated induction of heme oxygenase-1 in hepatoma cells. Role of mitogen-activated protein kinases. J. Biol.

Chem. 273, 8922-8931.
Fang, J., Sawa, T., Akaike, T., Akuta, T., Sahoo, S.K., Khaled, G., Hamada, A., Maeda, H. 2004. In vivo antitumor activity of pegylated zinc protoporphyrin: targeted inhibition of heme oxygenase in solid tumor. Cancer Res. 63, 3567-3574.
Fauconneau, B., Petegnief, V., Sanfeliu, C., Piriou, A., Planas, A. M. 2002. Induction of heat shock proteins (HSPs) by sodium arsenite in cultured astrocytes and reduction of hydrogen peroxide-induced cell death. J. Neurochem. 83, 1338-1348.
Fernando, P., Heikkila, J.J. 2000. Functional characterization of *Xenopus* small heat shock protein, Hsp30C : the carboxyl end is required for stability and chaperone activity. Cell Stress Chaperones 5, 148-159.
Galazyn-Sidorczuk, M., Brzoska, M.M., Jurczuk, M., Moniuszko-Jakoniuk, J. 2009. Oxidative damage to proteins and DNA in rats exposed to cadmium and/or ethanol. Chem. Biol. Interac. 180, 31-38.
Gellalchew, M., Heikkila, J.J. 2005. Intracellular localization of *Xenopus* small heat shock protein, hsp30, in A6 kidney epithelial cells. Cell. Biol. Int. 29, 221-227.
Gong, P., Hu, B., Cederbaum, A.I. 2004. Diallyl sulfide induces heme oxygenase-1 through MAPK pathway. Arch. Biochem. Biophys. 432, 252–260.
Gordon, S., Bharadwaj, S., Hnatov, A., Ali, A., Ovsenek, N. 1997. Distinct stress-inducible and developmentally regulated heat shock transcription factors in *Xenopus* oocytes. Dev. Biol. 181, 47-63.
Gornati, R., Monetti, C., vigetti, D., Bosisio, S., Fortaner, S., Sabbioni, E., Bernardini, G., Prati, M. 2002. Arsenic toxicity and HSP70 expression in *Xenopus laevis* embryos. Altern. Lab. Anim. 30, 597-603.
Gottlieb, Y., Truman, M., Cohen, L.A., Leichtmann-Bardoogo, Y., Meyron-Holtz, E.G. 2012. Endoplasmic reticulum anchored heme-oxygenase 1 faces the cytosol. Haematologica 97, 1489-1493.
Gozzelino, R., Jeney, V., Soares, M.P. 2010. Mechanisms of cell protection by heme oxygenase-1. Annu. Rev. Pharmacol. Toxicol. 50, 323-354.
Hanneken, A., Lin, F.F., Johnson, J., Maher, P. 2006. Flavonoids protect human retinal pigment epithelial cells from oxidative-stress-induced death. Invest. Opthalmol. Vis. Sci. 47, 3164-3177.
Hara, E., Takahashi, K., Tominaga, T., Kumabe, T., Kayama, T., Suzuki, H., Fujita, H., Yoshimoto, T., Shirato, K., Shibahara, S. 1996. Expression of heme oxygenase and inducible nitric oxide synthase mRNA in human brain tumors. Biochem. Biophys. Res. Commun. 224, 153–158.
Heikkila, J.J. 2004. Regulation and function of small heat shock protein genes during amphibian development. J. Cell. Biochem. 93, 672-680.
Heikkila, J.J. 2010. Heat shock protein gene expression and function in amphibian model systems. Comp. Biochem. Physiol. A. Mol. Integr. Physiol. 156, 19-33.
Hock, T.D., Nick, H.S., Agarwal, A. 2004. Upstream stimulatory factors, USF1 and USF2, bind to the human haem oxygenase-1 proximal promoter *in vivo* and regulate its transcription. Biochem. J. 383, 209-218.
Hough, R., Pratt, G., Rechsteiner, M. 1987. Purification of two high molecular weight proteases from rabbit reticulocyte lysate. J. Biol. Chem. 262, 8303–8313.
Huber, III, W.J. Scruggs, B.A., Backes, W.L. 2009. C-terminal membrane spanning region of human heme oxygenase-1 mediates a time-dependent complex formation with cytochrome P450 reductase. Biochemistry 48, 190-197.
Juan, S.H., Lee, T.S., Tseng, K.W., Liou, J.Y., Shyue, S.K., Wu, K.K., Chau, L.Y. 2001. Adenovirus-mediated heme oxygenase-1 gene transfer inhibits the development of atherosclerosis in apolipoprotein E-deficient mice. Circulation 104, 1519-1525.

Kastle, M., Woschee, E., Grune, T. 2012. Histone deacetylase 6 (HDAC6) plays a crucial role in p38MAPK-dependent induction of heme oxygenase-1 (HO-1) in response to proteasome inhibition. Free Radic. Biol. Med. 53, 2092-2101.

Katschinski, D.M. 2004. On heat and cells and proteins. News Physiol. Sci. 19, 11-15.

Keyse, S.M., Tyrrell, R. M. 1989. Heme oxygenase is the major 32-kDa stress protein induced in human skin fibroblasts by UVA radiation, hydrogen peroxide and sodium arsenite. Proc. Natl. Acad. Sci. USA 86, 99-103.

Khamis, I., Heikkila, J.J. 2013. Enhanced HSP30 and HSP70 accumulation in *Xenopus* cells subjected to concurrent sodium arsenite and cadmium chloride stress. Comp. Biochem. Physiol. C Toxicol. Pharmacol. 158, 165-172.

Khan, S., Rammeloo, A.W., Heikkila, J.J. 2012. Withaferin A induces proteasome inhibition, endoplasmic reticulum stress, the heat shock response and acquisition of thermotolerance. PLOS ONE. 7, e50547. doi: 10.1371/journal/pone.0050547.

Kirkpatrick, D.S., Dale, K.V., Catania, J.M., Gandolfi, A.J. 2003. Low-level arsenite causes accumulation of ubiquitinated proteins in rabbit renal cortical slices and HEK293 cells. Toxicol. Appl. Pharmacol. 186, 101-109.

Koizumi, S., Gong, P., Suzuki, K., Murata, M. 2007. Cadmium-responsive element of the human heme oxygenase-1 gene mediates heat shock factor 1-dependent transcriptional activation. J. Biol. Chem. 282, 8715-8723.

Lang, L., Miskovic, D., Lo, M., Heikkila J.J. 2000. Stress-induced, tissue-specific enrichment of hsp70 mRNA accumulation in *Xenopus laevis* embryos. Cell Stress Chaperones 5, 36-44.

Lau, A., Whitman, S.A., Jaramillo, M.C., Zhang, D.D. 2012. Arsenic-mediated activation of the Nrf2-Keap1 antioxidant pathway. J. Biochem. Molecular Toxicology. 27, 99-105.

Lee, D.H., Goldberg, A.L. 1998. Proteasome inhibitors: valuable new tools for cell biologists. Trends Cell Biol. 8, 397-403.

Lee, P.J., Alam, J., Wiegand, G.W., Choi, A.M.K. 1996. Overexpression of heme oygenase-1 in human pulmonary epithelial cells results in cell growth arrest and increased resistance to hyperoxia. Proc. Natl. Acad. Sci. USA 93, 10393-10398.

Lee, P.C., Ho, I.C., Lee, T.C. 2005. Oxidative stress mediates sodium arsenite-induced expression of heme oxygenase-1, monocyte chemoattractant protein-1, and interleukin-6 in vascular smooth muscle cells. Toxicol. Sci. 85, 541-550.

Li, W., Chou, I.N. 1992. Effects of sodium arsenite on the cytoskeleton and cellular glutathione levels in cultured cells. Toxicol. Appl. Pharmacol. 114, 132-139.

Linnenbaum, M., Busker, M., Kraehling, J.R., Behrends, S. 2012. Heme oxygenase isoforms differ in their subcellular trafficking during hypoxia and are differentially modulated by cytochrome P450 reductase. PLOS ONE. 7, e35483. doi: 10.1371/journal.pone.0035483.

Liu, X., Wei, J., Peng, D.H., Layne, M.D., Yet, S.F. 2005. Absence of heme oxygenase-1 exacerbates myocardial ischemia/reperfusion injury in diabetic mice. Diabetes. 54, 778-784.

Liu, J., Kadiiska, M.B., Liu, Y., Lu, T., Qu, W., Waalkes, M.P. 2001. Stress-related gene expression in mice treated with inorganic arsenicals. Toxicol. Sci. 61, 314-320.

Maines M.D., Abrahamsson, P.A. 1996. Expression of heme oxygenase-1 (HSP32) in human prostate: normal, hyperplastic, and tumor tissue distribution. Urology 47, 727–733.

Masuya, Y., Hioki, K., Tokunaga, R., Taketani, S. 1998. Involvement of the tyrosine phosphorylation pathway in induction of human heme oxygenase-1 by hemin, sodium arsenite, and cadmium chloride.

J. Biochem. 124, 628-633.
Martin, D., Rojo, A.I., Salinas, M., Diaz, R., Gallardo, G., Alam, J., Ruiz de Galarreta, C.M., Cuadrado, A. 2004. Regulation of heme oxygenase-1 expression through the phosphatidylinositol 3-kinase/Akt pathway and the Nrf2 transcription factor in response to the antioxidant phytochemical carnosol. J. Biol. Chem. 279, 8919-8929.
McGeachy, S.M., Dixon, D.G. 1989. The impact of temperature on the acute toxicity of arsenate and arsenite to rainbow trout (*Salmo gairdneri*). Exotoxicol. Environ. Saf. 17, 86-93.
Mendez-Armenta, M., Rios, C. 2007. Cadmium neurotoxicity. Environ. Toxicol. Pharmacol. 23, 350-358.
Mitani, K., Fujita, H., Sassa, S., Kappas, A. 1990. Activation of heme oxygenase and heat shock protein 70 genes by stress in human hepatoma cells. Biochem. Biophys. Res. Commun. 166, 1429-1434.
Miyamoto, Y., Ohshida, K., Sasago, K. 2009. Protein assay for heme oxygenase-1 (HO-1) induced by chemicals in HepG2 cells. J. Toxicol. Sci. 34, 709-714.
Morimoto, R.I. 1998. Regulation of the heat shock transcriptional response: Cross talk between a family of heat shock factors, molecular chaperones, and negative regulators. Genes Dev. 12, 3788-3796.
Morimoto, R.I. 2008. Proteotoxic stress and inducible chaperone networks in neurodegenerative diseases and aging. Genes Dev. 22, 1427-1438.
Morita, T., Mitsialis, S.A., Koike, H., Liu, Y., Kourembanas, S. 1997. Carbon monoxide controls the proliferation of hypoxic smooth muscle cells. J. Biol. Chem. 272, 32804-32809.
Mouchet, F., Baudrimont, M., Gonzalez, P., Cuenot, Y., Bourdineaud, J.P., Boudou, A., Gauthier, L. 2006. Genotoxic and stress inductive potential of cadmium in *Xenopus laevis* larvae. Aquat. Toxicol. 78, 157-166.
Okinaga, S., Takahashi, K., Takeda, K., Yoshizawa, M., Fujita, H., Sasaki, H., Shibahara, S. 1996. Regulation of human heme oxygenase-1 gene expression under thermal stress. Blood. 87, 5074-5084.
Pappolla, M.A., Chyan, Y.J., Omar, R.A., Hsiao, K., Perry, G., Smith, M.A., Bozner, P. 1998. Evidence of oxidative stress and in vivo neurotoxicity of beta-amyloid in a transgenic mouse model of Alzheimer's disease: a chronic oxidative paradigm for testing antioxidant therapies in vivo. Am. J. Pathol. 152, 871-877.
Plowman, M.C., Grbac-Ivankovic, S., Martin, J., Hopfer, S.M., Sunderman, F.W.Jr. 1994. Malformations persist after metamorphosis of *Xenopus laevis* tadpoles exposed to Ni2+, Co2+, or Cd2+ in FETAX assays. Teratog. Carcinog. Mutagen. 14, 135-144.
Raju, V.S., Maines, M.D. 1994. Coordinated expression and mechanism of induction of HSP32 (heme oxygenase-1) mRNA by hyperthermia in rat organs. Biochim. Biophys. Acta. 1217, 273-280.
Reichard, J.F., Sartor, M.A., Puga, A. 2008. BACH1 is a specific repressor of HMOX1 that is inactivated by arsenite. J. Biol. Chem. 283, 22363-22370.
Ryter, S.W., Alam, J., Choi, A.M. 2006. Heme oxygenase-1/carbon monoxide: from basic science to therapeutic applications. Physiol. Rev. 86, 583-650.
Samuel, S. Kathirvel, R., Jayavelu, T., Chinnakkannu, P. 2005. Protein oxidative damage in arsenic induced rat brain: influence of DL-alpha-lipoic acid. Toxicol. Lett. 15, 27-34.
Saydam, N., Steiner, F., Georgiev, O., Schaffner, W. 2003. Heat and heavy metal stress synergize to mediate transcriptional hyperactivation by metal-responsive transcription factor MTF-1. J. Biol. Chem. 278, 31879-31883.
Schipper, H.M., Liberman, A., Stopa, E.G. 1998. Neural heme oxygenase-1 expression in idiopathic Parkinson's disease. Exp. Neurol. 150, 60–68.

Seo, W.Y., Goh, A.R., Ju, S.M., Song, H.Y., Kwon, D-J., Jun, J-G., Kim, B.C., Choi, S.Y., Park, J. 2011. Celastrol induces expression of heme oxygenase-1 through ROS/Nrf2/ARE signaling in the HaCaT cells. Biochem. Biophys. Res. Commun. 407, 535-540.

Sharma, B., Patino, R. 2008. Exposure of *Xenopus laevis* tadpoles to cadmium reveals concentration-dependent bimodal effects on growth and monotonic effects on development and thyroid gland activity. Toxicol. Sci. 105, 51-58.

Shi, J., Mei, W., Yang, J. 2008. Heme metabolism enzymes are dynamically expressed during Xenopus embryonic development. Bio. Cell. 32, 259-263.

Sikorski, E.M., Uo, T., Morrison, R.S., Agarwal, A. 2006. Pescadillo interacts with the cadmium response element of the human heme oxygenase-1 promoter in renal epithelial cells. J. Biol. Chem. 281, 24423-30.

Smith, M.A., Kutty, R.K., Richey, P.L., Yan, S.D., Stern, D., Chader, G.J., Wiggert, B., Petersen, R.B., Perry, G. 1994. Heme oxygenase-1 is associated with the neurofibrillary pathology of Alzheimer's disease. Am. J. Pathol. 145, 42–47.

Søfteland, L., Holen, E., Olsvik, P.A. 2010. Toxicological application of primary hepatocyte cell cultures of Atlantic cod (*Gadus morhua*): Effects of BNF, PCDD and Cd. Comp. Biochem. Physiol. C Toxicol. Pharmacol. 151, 401-411.

Souza, V., Bucio, L., Gutierrez-Ruiz, M.C. 1997. Cadmium uptake by a human hepatic cell line (WRL-68 cells). Toxicology 120, 215-220.

Stewart, D., Killeen, E., Naquin, R., Alam, S., Alam, J. 2003. Degradation of transcription factor Nrf2 via the ubiquitin-proteasome pathway and stabilization by cadmium. J. Biol. Chem. 278, 2396-2302.

Suzuki, H., Tashiro, S., Sun, J., Doi, H., Satomi, S., Igarashi, K. 2003. Cadmium induces nuclear export of Bach1, a transcriptional repressor of heme oxygenase-1 gene. J. Biol. Chem. 278, 49246-49253.

Takahashi, M., Dore, S., Ferris, C.D., Tomita, T., Sawa, A., Wolosker, S.S., Snyder, S.H. 2000. Amyloid precursor proteins inhibit heme oxygenase activity and augment neurotoxicity in Alzheimer's disease. Neuron 28, 461-473.

Takeda, K., Fujita, H., Shibahara, S. 1995. Differential control of the metal-mediated activation of the human heme oxygenase-1 and metallothionein IIA genes. Biochem. Boiphys. Res. Commun. 207, 160-167.

Taketani, S., Kohno, H., Yoshinaga, T., Tokunaga, R. 1988. Induction of heme oxygenase in rat hepatoma cells by exposure to heavy metals and hyperthermia. Biochem. Int. 17, 665-672.

Taketani, S., Kohno, H., Yoshinaga, T., Tokunaga, R. 1989. The human 32-kDa stress protein induced by exposure to arsenite and cadmium ions is heme oxygenase. FEBS Lett. 245, 173-176.

Teng, Y.C., Tai, Y.I., Lee, Y.H., Lin, A.M. 2013. Role of HO-1 in the arsenite-induced neurotoxicity inprimary cultured cortical neurons. Mol. Neurobiol. 438, 281-287.

Tozawa, K., Sakurada, S., Kohri, K., Okamoto, T. 1995. Effects of anti-nuclear factor kappa B reagents in blocking adhesion of human cancer cells to vascular endothelial cells. Cancer Res. 55, 4162–4167.

Turkseven, S., Kruger, A., Mingone, C.J., Kaminski, P., Inaba, M., Rodella, L.F., Ikehara, S., Wolin, M.S., and Abraham, N.G. 2005. Antioxidant mechanism of heme oxygenase-1 involves an increase in superoxide dismutase and catalase in experimental diabetes. Am. J. Physiol. Heart Circ. Physiol. 289, H701-707.

Voyer, J., Heikkila, J.J. 2008. Comparison of the effect of heat shock factor inhibitor, KNK437, on heat shock- and chemical stress-induced hsp30 gene expression in *Xenopus laevis* A6 cells. Comp. Biochem. Physiol. A Mol. Integr. Physiol. 151, 253-261.

Waisberg, M., Pius, J., Hale, B., Beyersmann, D. 2003. Molecular and cellular mechanisms of cadmium

carcinogenesis. Toxicology 192, 95-117.
Walcott, S.E., Heikkila, J.J. 2010. Celastrol can inhibit proteasome activity and upregulate the expression of heat shock protein genes, hsp30 and hsp70, in *Xenopus laevis* A6 cells. Comp. Biochem. Physiol. A. Mol. Integr. Physiol. 156, 285-293.
Williams, C.R., Gallagher, E.P. 2013. Effects of cadmium on olfactory mediated behaviors and molecular biomarkers in coho salmon (*Oncorhynchus kisutch*). Aquat. Toxicol. 140-141, 295-302.
Woolfson, J.P., Heikkila, J.J. 2009. Examination of cadmium-induced expression of the small heat shock protein gene, hsp30, in *Xenopus laevis* A6 kidney epithelial cells. Comp. Biochem. Physiol. A Mol. Integr. Physiol. 152, 91-99.
Wu, W.T., Chi, K.H., Ho, F.M., Tsao, W.C., Lin, W.W. 2004. Proteasome inhibitors up-regulate haem oxygenase-1 gene expression: requirement of p38 MAPK (mitogen-activated protein kinase) activation but not of NF-kappaB (nuclear factor kappaB) inhibition. Biochem. J. 379, 587-593.
Yamamoto, N., Izumi, Y., Matsuo, T., Wakita, S., Kume, T., Takada-Takatori, Y., Sawada, H., Akaike, A. 2010. Elevation of heme oxygenase-1 by proteasome inhibition afforbs dopaminergic neuroprotection. J. Neurosci. Res. 88, 1934-1942.
Yoshida, T., Biro, P., Cohen, T., Muller, R.M., Shibahara, S. 1988. Human heme oxygenase cDNA and induction of its mRNA by hemin. Eur. J. Biochem. 171, 457-461.
Young, J.T.F., Heikkila, J.J. 2010. Proteasome inhibition induces hsp30 and hsp70 gene expression as well as the acquisition of thermotolerance in *Xenopus laevis* A6 cells. Cell Stress Chaperones 15, 323-334.
Young, J.T.F., Gauley, J., Heikkila, J.J. 2009. Simultaneous exposure of *Xenopus* A6 kidney epithelial cells to concurrent mild sodium arsenite and heat stress results in enhanced hsp30 and hsp70 gene expression and the acquisition of thermotolerance. Comp. Biochem. Physiol. A. Mol. Int. Physiol. 153, 417-424.
Yu, X., Hong, S., Faustman, E.M. 2008. Cadmium-induced activation of stress signaling pathways, disruption of ubiquitin-dependent protein degradation and apoptosis in primary rat Sertoli cell-gonocyte cocultures. Toxicol. Sci. 104, 385-396.
Yu, X., Robinson, J.F., Sidhu, J.S., Hong, S., Faustman, E.M. 2010. A system-based comparison of gene expression reveals alterations in oxidative stress, disruption of ubiquitin-proteasome system and altered cell cycle regulation after exposure to cadmium and methylmercury in mouse embryonic fibroblast. Toxicol. Sci. 114, 356-377.
Yu, X., Tao, W., Jiang, F., Li, C., Lin, J., Liu, C. 2010. Celastrol attenuates hypertension-induced inflammation and oxidative stress in vascular smooth muscle cells via induction of heme oxygenase-1. Am. J. Hypertens. 23, 895-903.

Figure Legends

Figure 1. Amino acid sequence of *Xenopus laevis* HO-1. The *X. laevis* HO-1 protein (Genbank accession number: NP_001089909), which is 291 amino acids long has a putative heme ligand binding site, a conserved histidine residue (H28), that is indicated by an asterisk below the letter. The putative heme binding pocket residues are shown in a bold font and underlined. The HO-1 antibody (Enzo Life Sciences) used in this study, which was produced against a synthetic human HO-1 peptide, shares 100% sequence identity with the corresponding *X. laevis* HO-1 amino acids

(D15-H28) indicated by the solid line. The conserved region that was compared with other organisms for shared identity in Table 1 is indicated with a dashed line spanning P129 to R186.

Figure 2. Effect of heat shock on HO-1 accumulation. A6 cells were maintained at 22 °C (C) or incubated at 30, 33 or 35 °C for 2 h followed by a 2 h recovery at 22 °C. Some cells were also treated with 20 μM sodium arsenite (As) at 22 °C for 24 h. Cells were harvested and total protein was isolated. Forty micrograms of total protein was subjected to immunoblot analysis using anti-HO-1, anti-HSP30 and anti-actin antibodies as described in Materials and methods. These results are representative of 3 separate experiments.

Figure 3. Effect of different concentrations of sodium arsenite or cadmium chloride on HO-1 accumulation. Cells were maintained at 22 °C (C) or incubated with 5, 10, 20, 30 or 50 μM sodium arsenite (As; panel A) or with 25, 50, 100 or 200 μM cadmium chloride (Cd; panel C) at 22 °C for 24 h. After treatment, total protein was isolated and subjected to immunoblot analysis as detailed in Materials and methods. These results are representative of 3 separate experiments. Densitometric analysis of the band intensity for HO-1 (black) and HSP30 (white) employed Image J software (panels B and D). The results were expressed as a percentage of the maximum band intensity acquired for each protein in each trial (panel B: 10 μM As for HO-1 and 30 μM for HSP30; panel D: 100 μM Cd for both HO-1 and HSP30). Vertical error bars denote standard error. A one-way ANOVA with a Tukey's Multiple Comparisons post-test was used to determine significance. Significant differences between the control cells and treated cells are indicated as * ($p < 0.05$).

Figure 4. Time course of As- or Cd-induced HO-1 accumulation. Cells were maintained at 22 °C (C) or incubated with 30 μM As (panel A) or 100 μM Cd (panel C) at 22 °C for 4, 8, 12, 24 or 48 h. After treatment, total protein was isolated and analyzed by immunoblot analysis. These results are representative of 3 separate experiments. B) Densitometric analysis of the band intensity for HO-1 (black) and HSP30 (white) utilized Image J software (panels B and D). The results were expressed as a percentage of the maximum band intensity acquired for each protein in each trial (panel B: 48 h for both HO-1 and HSP30; panel D: 48 h for both HO-1 and HSP30) as described in the legend of Figure 3. Significant differences between control and treated cells are indicated as * ($p < 0.05$).

Figure 5. Effect of actinomycin D and cycloheximide treatment on As- and Cd-induced HO-1 accumulation. A) Cells were incubated at 22 °C (C) or treated with 30 μM As or 100 μM Cd for 12 h at 22 °C, with or without a 30 min pretreatment with 2 or 5 μg/mL actinomycin D. B) Cells were incubated at 22 °C (C) or treated with 30 μM As for 24 h or 100 μM Cd for 12 h at 22 °C, with or without a 6 h pretreatment with 100 μM cycloheximide (CHX). After these treatments, total protein

was isolated and subjected to immunoblot analysis as detailed in Materials and methods. These results are representative of 2 separate trials.

Figure 6. Effect of heat shock, As or Cd on the cellular localization of HO-1. A6 cells were cultured on base-washed glass coverslips and then maintained at 22 °C (C), heat shocked at 33 °C for 2 h with 2 h recovery or treated with 10 μM As or 100 μM Cd for 24 h. Actin and nuclei staining utilized phalloidin conjugated to TRITC (red) or DAPI (blue), respectively. HO-1 was detected with rabbit anti-HO-1 antibody, and a secondary antibody conjugated to Alexa-488 (green). The columns, from left to right, show the fluorescence detection channels for actin, HO-1, and combined actin, DAPI, and HO-1, respectively. The laser scanning confocal microscopy (LSCM) procedure was followed as outlined in the Materials and methods. White arrows indicate the presence of large HO-1 staining complexes in As-treated cells. The 20 μm scale bars are indicated at the bottom right corner of each panel.

Figure 7. HO-1 accumulation during recovery from As treatment in the absence or presence of cycloheximide. Cells were maintained at 22 °C (C) or subjected to 30 μM As treatment for 24 h and then allowed to recover for 0 to 48 h in fresh media at 22 °C in the absence (panel A) or presence of 100 μM cycloheximide (CHX; panel B). After treatment, total protein was isolated and analyzed by immunoblotting as described in Materials and methods. Densitometric analysis of the band intensity for HO-1 (black) and HSP30 (white) employed Image J software as described in the legend of Figure 3. The results were expressed as a percentage of the maximum band intensity acquired with each protein in each trial (panel A: 12 h As recovery time point for HO-1 and HSP30; panel B: 0 h As recovery time point for HO-1 and 4 h for HSP30). In both panels A and B, the data are the results of 3 separate trials. Significant differences between the control cells and treated cells are indicated as * ($p < 0.05$).

Figure 8. Effect of As or Cd on HO-1 accumulation with or without a mild heat shock. Cells were maintained at 22 °C (C) or incubated with 10 μM As or 10 μM Cd at either 22 or 30 °C for 12 h. In other experiments, cells were treated with 10 μM As and 10 μM Cd simultaneously at 22 °C for 12 h. After treatment, total protein was isolated and subjected to immunoblot analysis as described in Materials and methods. The data are representative of 3 separate experiments. Densitometric analysis of the band intensity for HO-1 (black) and HSP30 (white) utilized Image J software as mentioned in the legend of Figure 3. The results were expressed as a percentage of the maximum band intensity acquired for each protein in each trial (10 μM As plus 30 °C for both HO-1 and HSP30). Significant differences between the control cells and treated cells are indicated as * ($p < 0.05$).

Figure 9. Effect of different MG132 concentrations and treatment times on HO-1 accumulation. Cells were maintained at 22 °C or incubated with 5, 10, 20, or 30 μM MG132 (panel A) at 22 °C for 24 h, or with 30 μM of MG132 at 22 °C for 0, 4, 8, 12, 24, or 48 h (panel C). Following treatment, total protein was isolated and subjected to immunoblot analysis. The immunoblots are representative of 3 separate experiments. In panels B and D, densitometric analysis of the band intensity for HO-1 (black) and HSP30 (white) employed Image J software. The results were expressed as a percentage of the maximum band intensity acquired for each protein in each trial (panel B: 20 μM MG132 for both HO-1 and HSP30; panel D: 48 h for both HO-1 and HSP30). Significant differences between the control cells and treated cells are indicated as * ($p < 0.05$).

Figure 10. Withaferin A and celastrol induced HO-1 accumulation occurred in a time-dependent manner. Cells were maintained at 22 °C (C) or treated with 5 μM withaferin A (WA; panel A) or 2.5 μM celastrol (CEL; panel B) for 2 to 24 h at 22 °C. Cells were harvested and total protein was isolated. Forty μg of the different protein samples were analyzed by immunoblot analysis as described in Material and methods. These data are representative of three separate experiments. Image J software was used to perform densitometric analysis of the signal intensity for HO-1 (black) or HSP30 (white) protein bands as described in Materials and methods and the legend of Figure 3. The data are expressed as a percentage of the maximum signal (panel B: 5 μM WA for 16 h for HO-1 or 5 μM WA for 24 h for HSP30; panel D: 2.5 μM celastrol for 24 h for HO-1 and HSP30). The standard error is represented by vertical error bars. Significant differences between the control and WA- or CEL-treated cells are indicated as * ($p < 0.05$).

Figure 11. Effect of MG132, WA or CEL on the localization of HO-1 in A6 cells. Cells were cultured on base-washed glass coverslips and maintained at 22 °C (Control) or treated with 20 μM MG132, 2.5 μM CEL, or 5 μM WA at 22 °C for 24 h. Actin and nuclei were stained directly with phalloidin conjugated to TRITC (red) or DAPI (blue), respectively. HO-1 was indirectly detected with an anti-HO-1 antibody and a secondary antibody conjugated to Alexa-488 (green). From left to right the columns display fluorescence detection channels for actin, HO-1 and merger of actin, DAPI and HO-1. The 20-μm white scale bars are indicated at the bottom right section of each panel. These results are representative of 3 different experiments.

Table 1. A comparison of *Xenopus laevis* HO-1, HO-2, and selected HO-1 homologues from other vertebrates.

Protein / Species	**% identity (complete amino acid sequence)**	**% identity (conserved region)**
HO-1 / *Xenopus tropicalis*	91	100
HO-1 / *Gallus gallus*	63	91
HO-1 / *Anas platyrhynchos*	63	91
HO-1 / *Homo sapiens*	61	88
HO-1 / *Mus musculus*	59	84
HO-1 / *Alligator mississipiensis*	58	88
HO-2 / *Xenopus laevis*	53	74
HO-1 / *Danio rerio*	45	69

The sequences were obtained from the GenBank database (www.ncbi.nlm.nih.gov). The NCBI reference sequences of the proteins are: *Xenopus laevis* HO-1, **NP_001089909**; *Xenopus tropicalis* HO-1, **XP_002934766**; *Gallus gallus* HO-1, **ADK26061**; *Anas platyrhynchos* HO-1, **XP_005015402**; *Homo sapiens* HO-1, **ADZ76424**; *Mus musculus* HO-1, **EDL10826**; *Alligator mississipiensis* HO-1, **XP_006261961**; *Xenopus laevis* HO-2, **NP_001085675**, and *Danio rerio* HO-1, **NP_001120988**. The percent identity of a highly conserved region (residues P129 – R186 in *Xenopus laevis* HO-1) was also determined using these data. This domain is indicated with a dashed line in Figure 1.

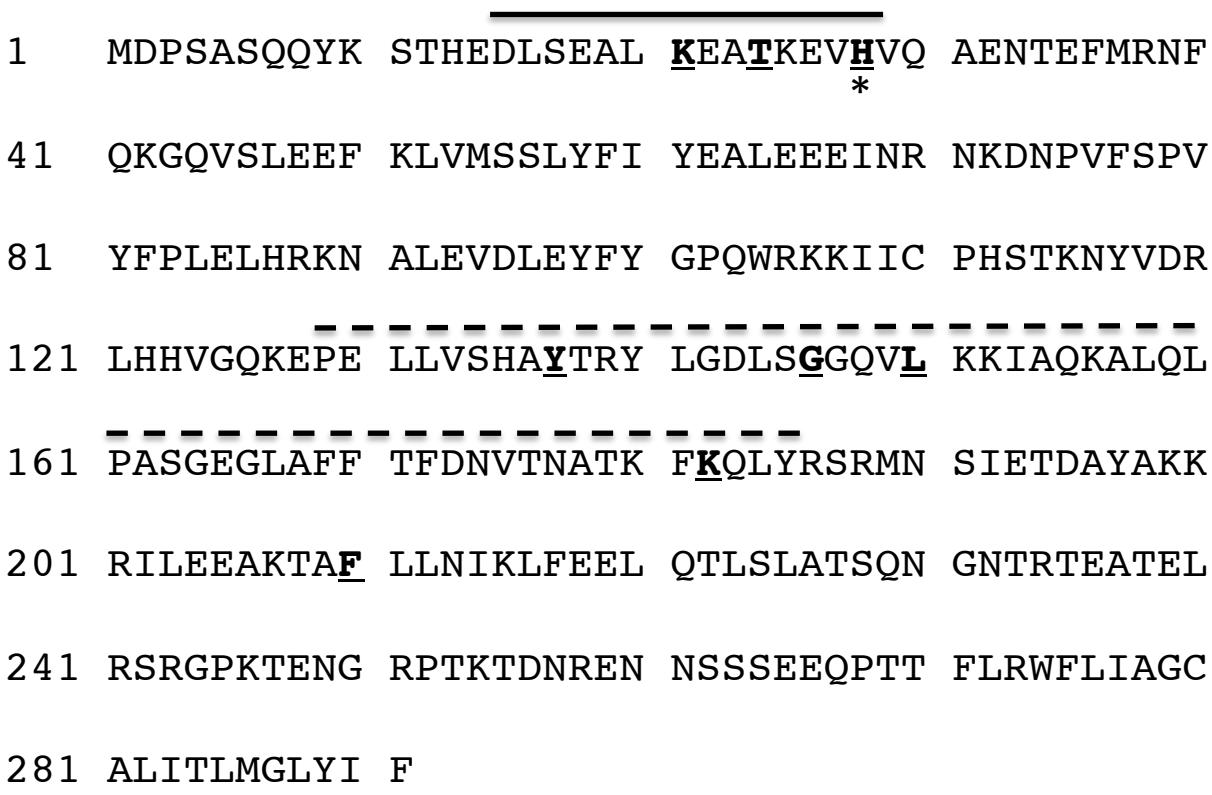
1 MDPSASQQYK STHEDLSEAL KEATKEVHVQ AENTEFMRNF
41 QKGQVSLEEF KLVMSSLYFI YEALEEEINR NKDNPVFSPV
81 YFPLELHRKN ALEVDLEYFY GPQWRKKIIC PHSTKNYVDR
121 LHHVGQKEPE LLVSHAYTRY LGDLSGGQVL KKIAQKALQL
161 PASGEGLAFF TFDNVTNATK FKQLYRSRMN SIETDAYAKK
201 RILEEAKTAF LLNIKLFEEL QTLSLATSQN GNTRTEATEL
241 RSRGPKTENG RPTKTDNREN NSSSEEQPTT FLRWFLIAGC
281 ALITLMGLYI F

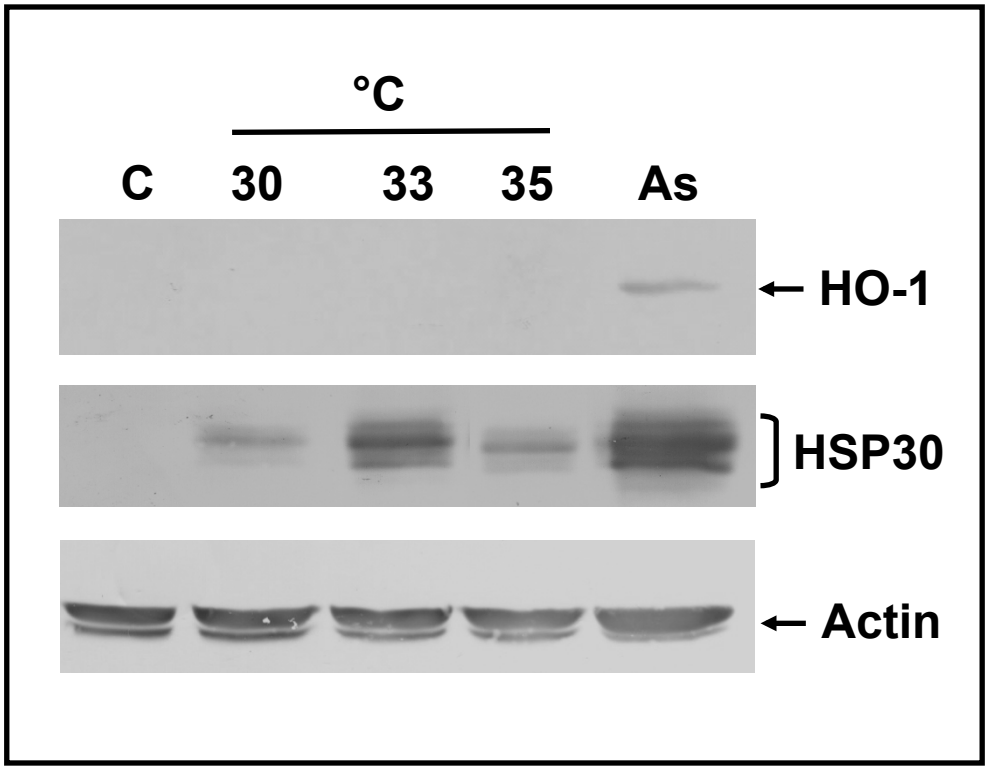
°C
C
30
33
35
As
← HO-1
HSP30
← Actin

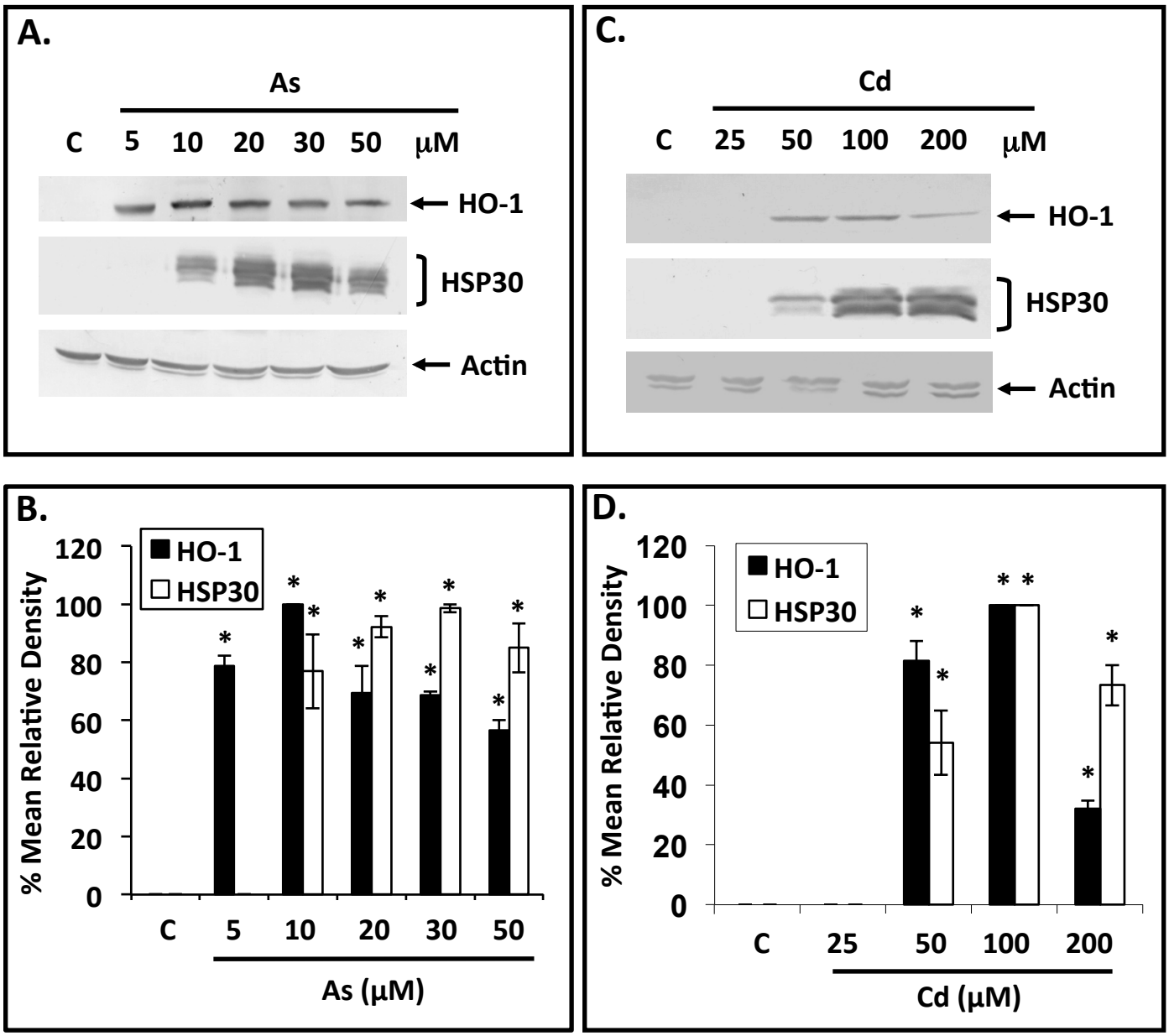
A.
As
C 5 10 20 30 50 μM
HO-1
HSP30
Actin
C.
Cd
C 25 50 100 200 μM
HO-1
HSP30
Actin
B.
HO-1
HSP30
% Mean Relative Density
120
100
80
60
40
20
0
C 5 10 20 30 50
As (μM)
D.
HO-1
HSP30
% Mean Relative Density
120
100
80
60
40
20
0
C 25 50 100 200
Cd (μM)

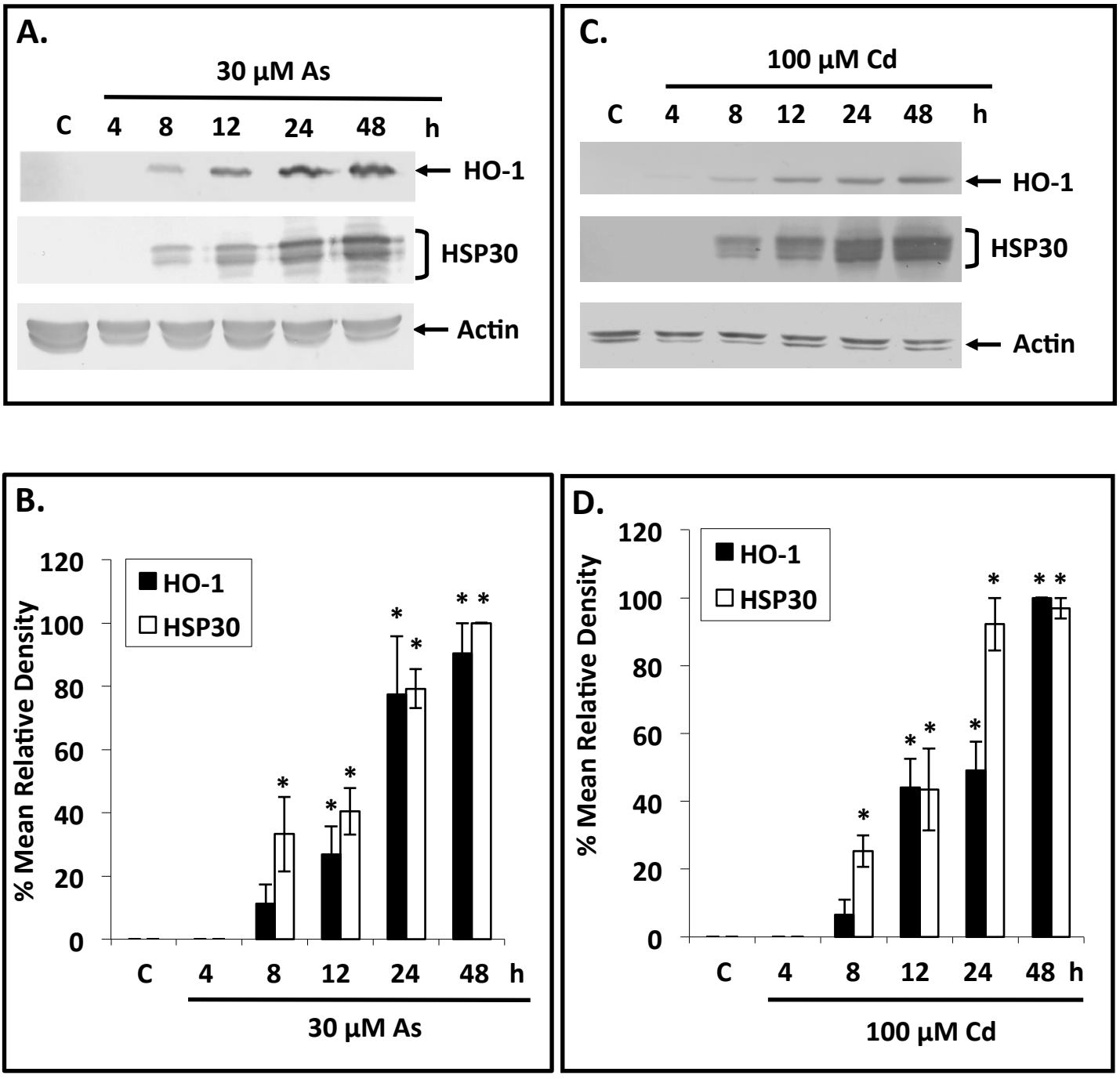
A.
30 µM As
C 4 8 12 24 48 h
HO-1
HSP30
Actin
C.
100 µM Cd
C 4 8 12 24 48 h
HO-1
HSP30
Actin
B.
% Mean Relative Density
HO-1
HSP30
C 4 8 12 24 48 h
30 µM As
D.
% Mean Relative Density
HO-1
HSP30
C 4 8 12 24 48 h
100 µM Cd

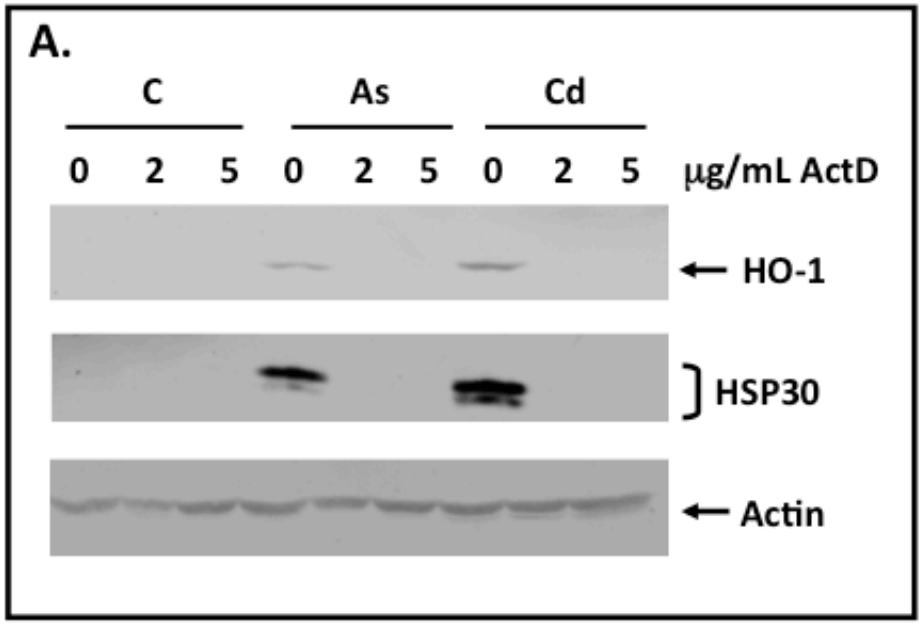
A.
C
As
Cd
0 2 5 0 2 5 0 2 5
μg/mL ActD
HO-1
HSP30
Actin

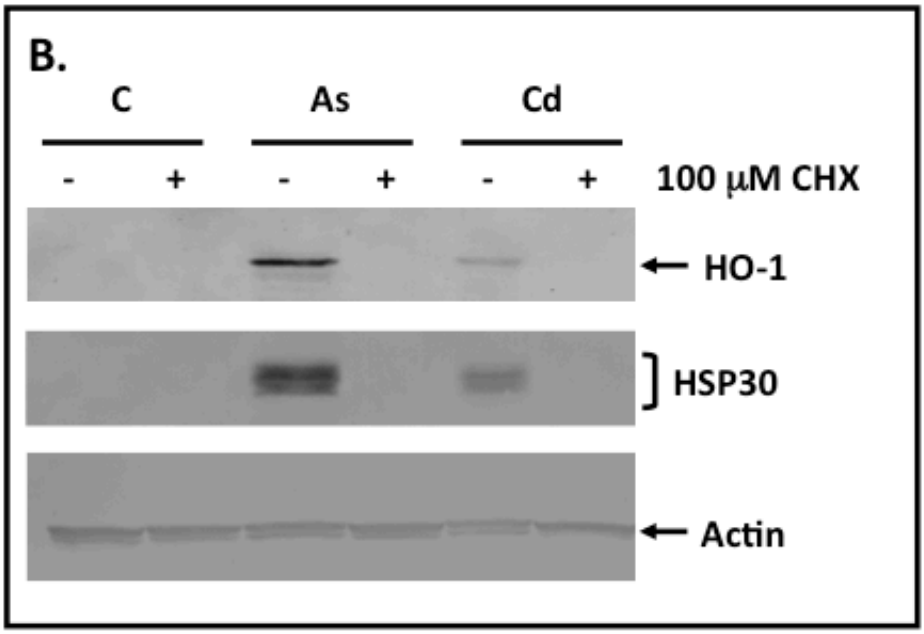
B.
C
As
Cd
- + - + - +
100 μM CHX
HO-1
HSP30
Actin

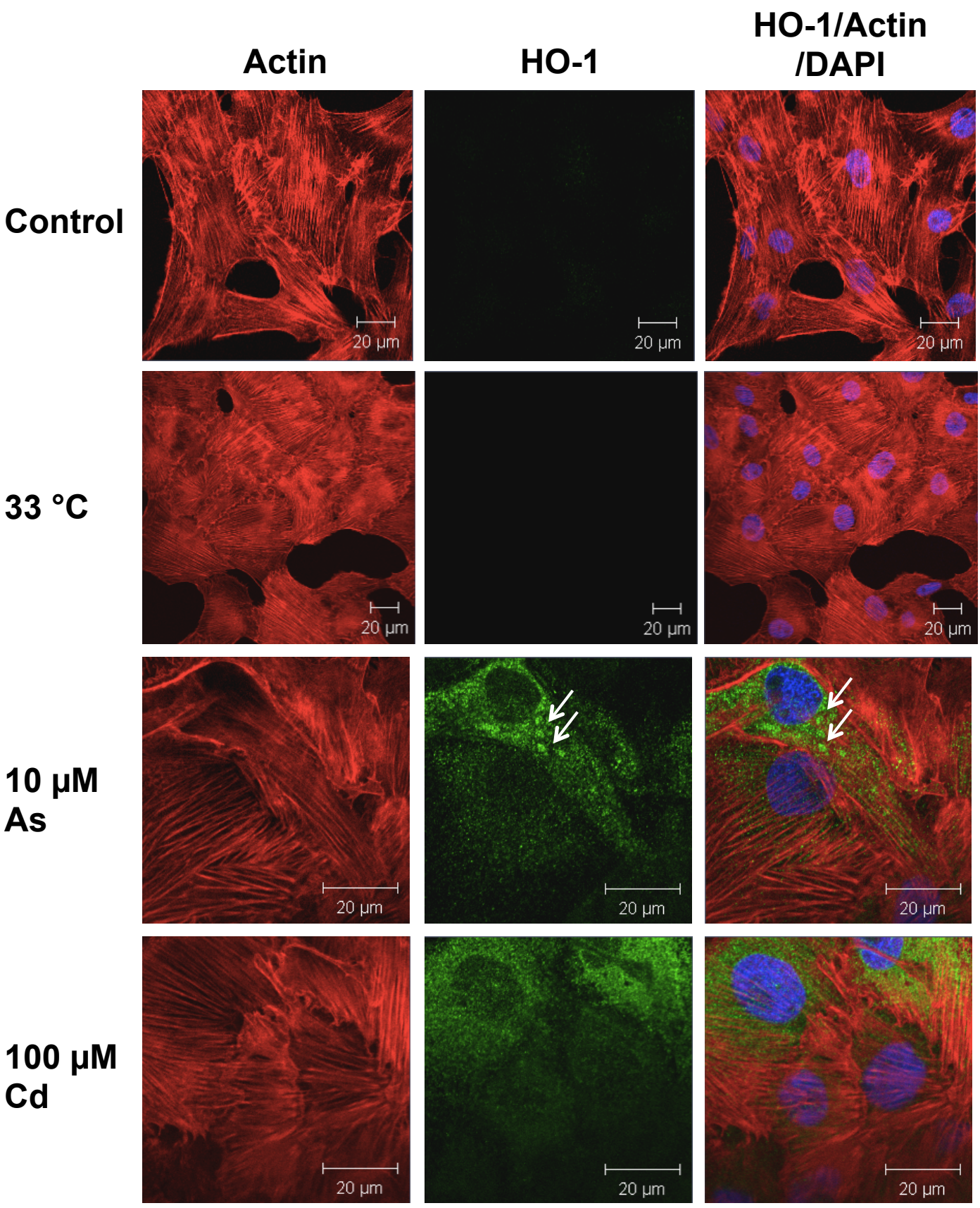
Actin
HO-1
HO-1/Actin /DAPI
Control
33 °C
10 µM As
100 µM Cd
20 µm

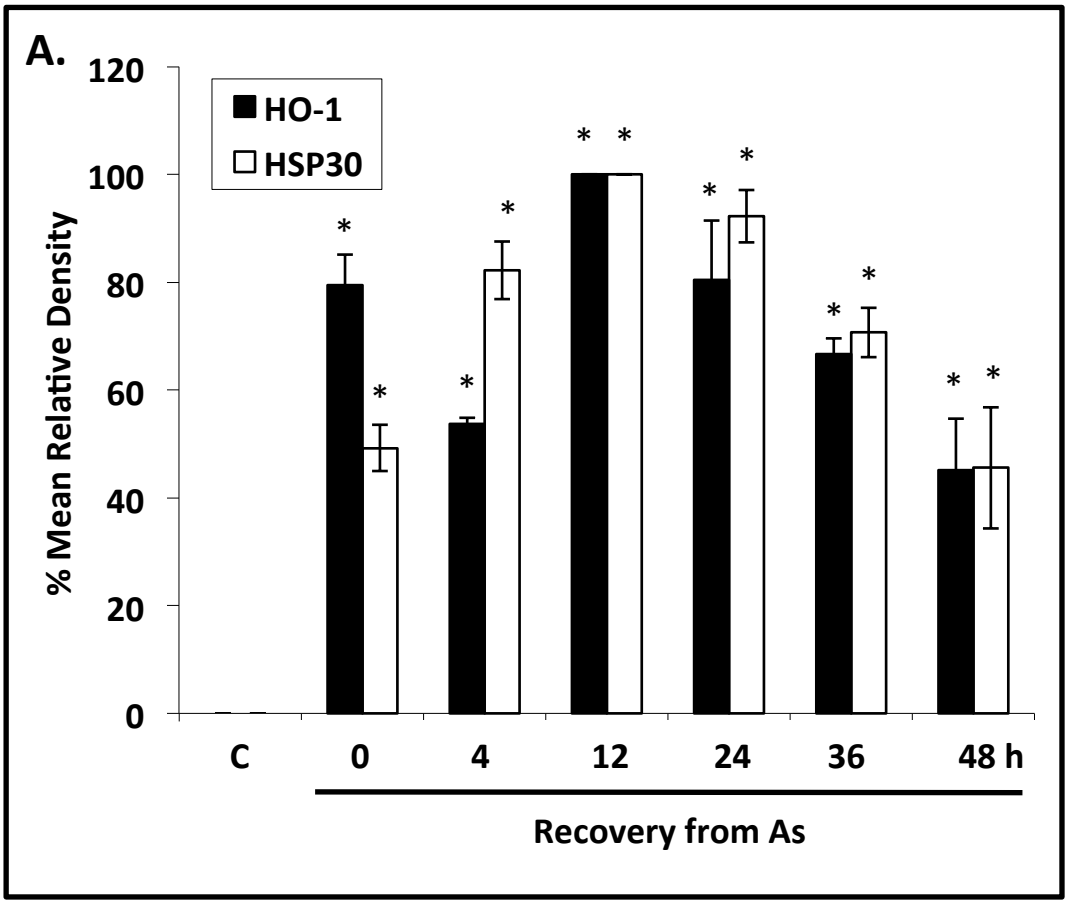
A.
HO-1
HSP30
% Mean Relative Density
120
100
80
60
40
20
0
C
0
4
12
24
36
48 h
Recovery from As

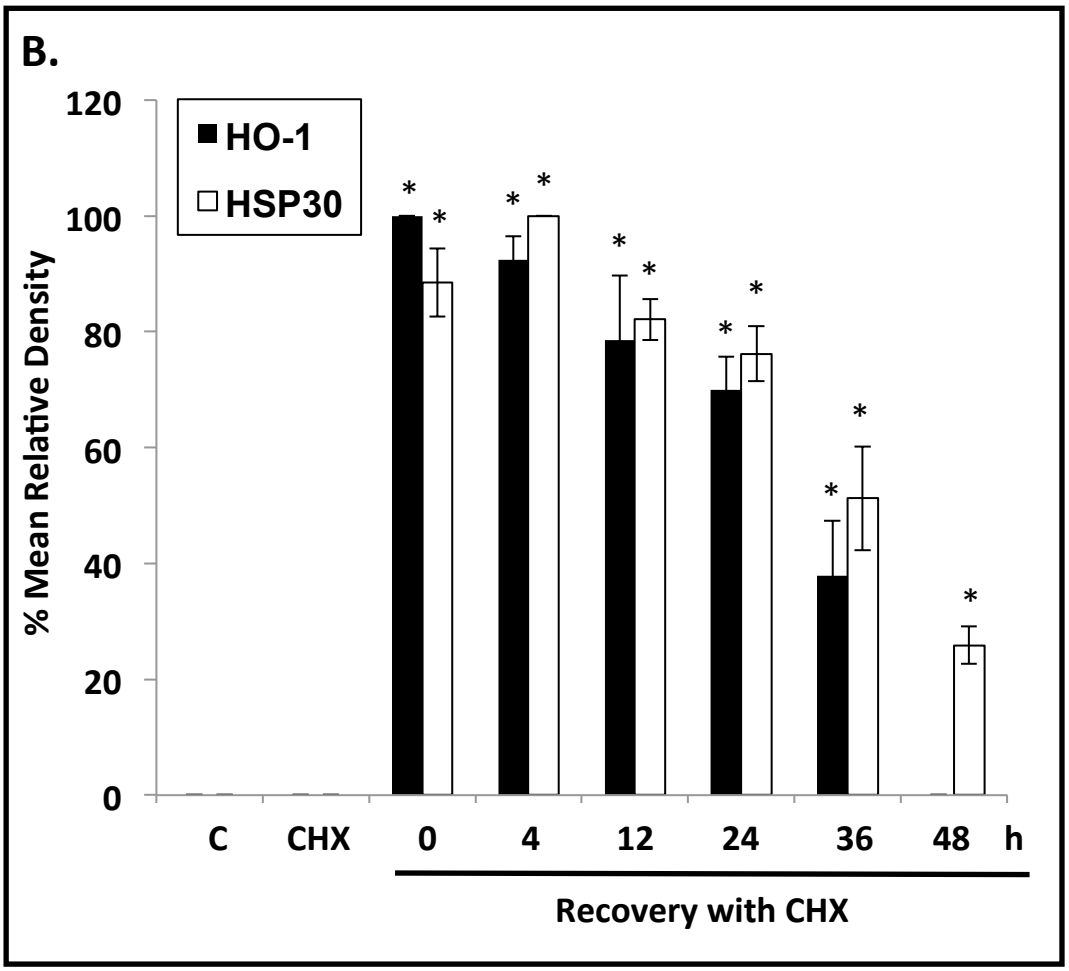
B.
HO-1
HSP30
% Mean Relative Density
120
100
80
60
40
20
0
C
CHX
0
4
12
24
36
48
h
Recovery with CHX

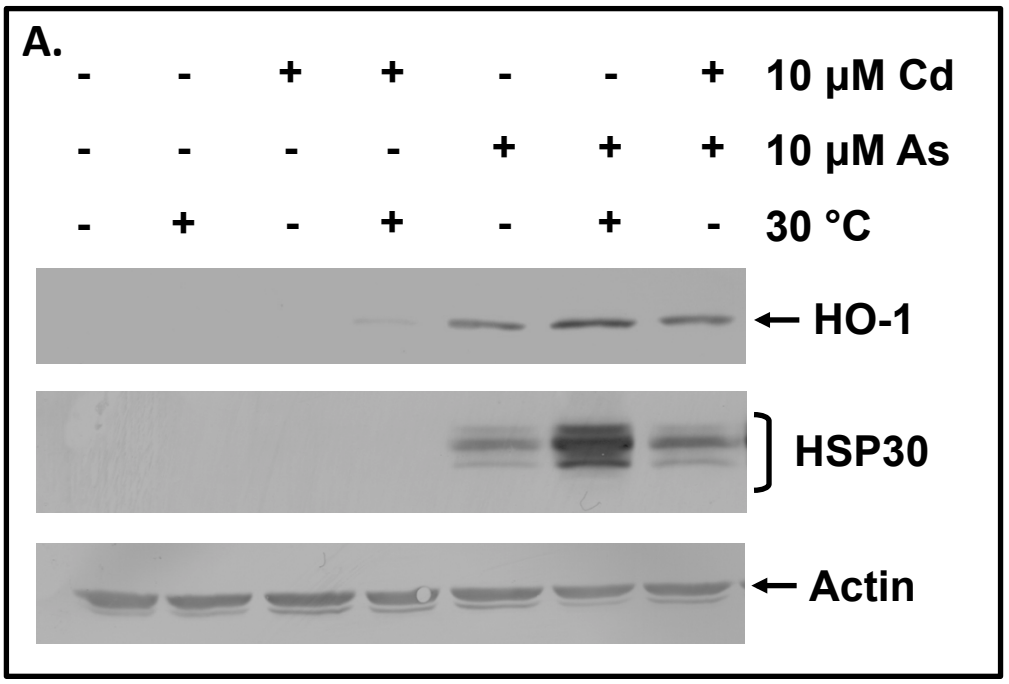
A.
- - + + - - + 10 μM Cd
- - - - + + + 10 μM As
- + - + - + - 30 °C
← HO-1
HSP30
← Actin

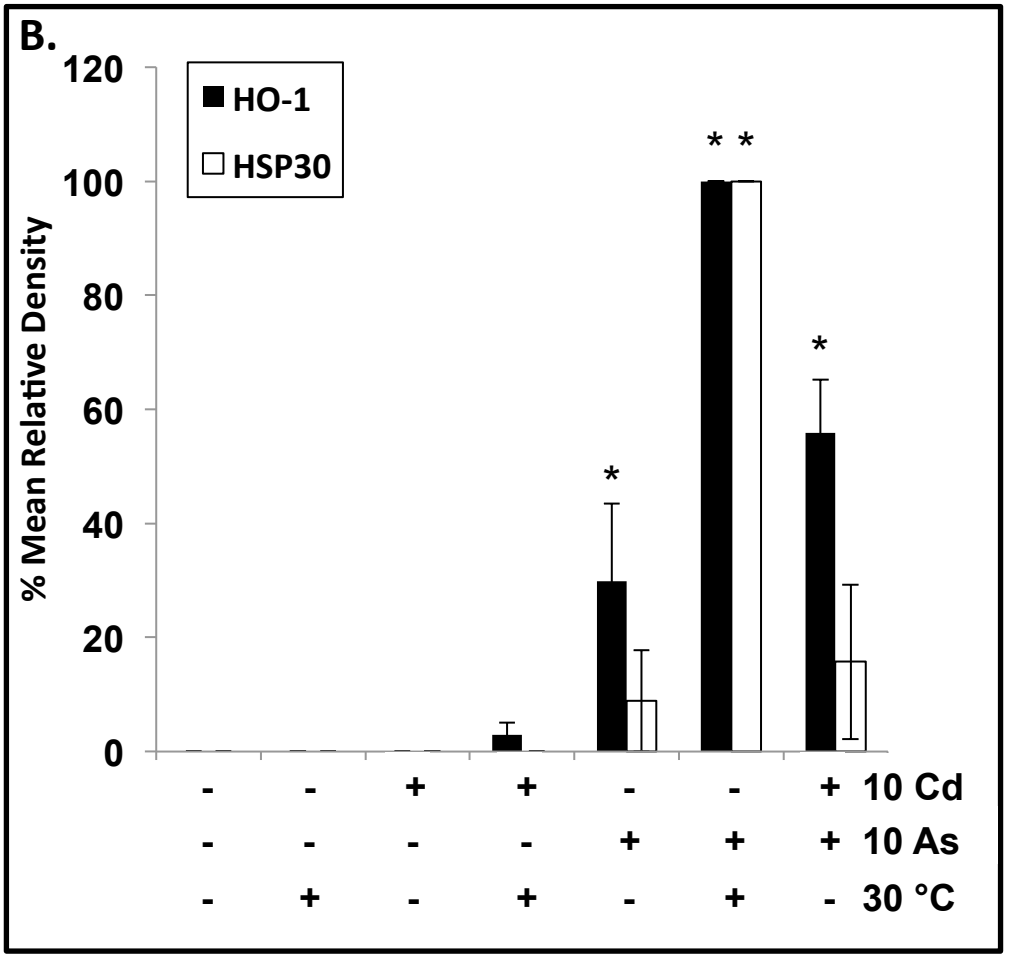
B.
HO-1
HSP30
% Mean Relative Density
120
100
80
60
40
20
0
* *
*
*
- - + + - - + 10 Cd
- - - - + + + 10 As
- + - + - + - 30 °C

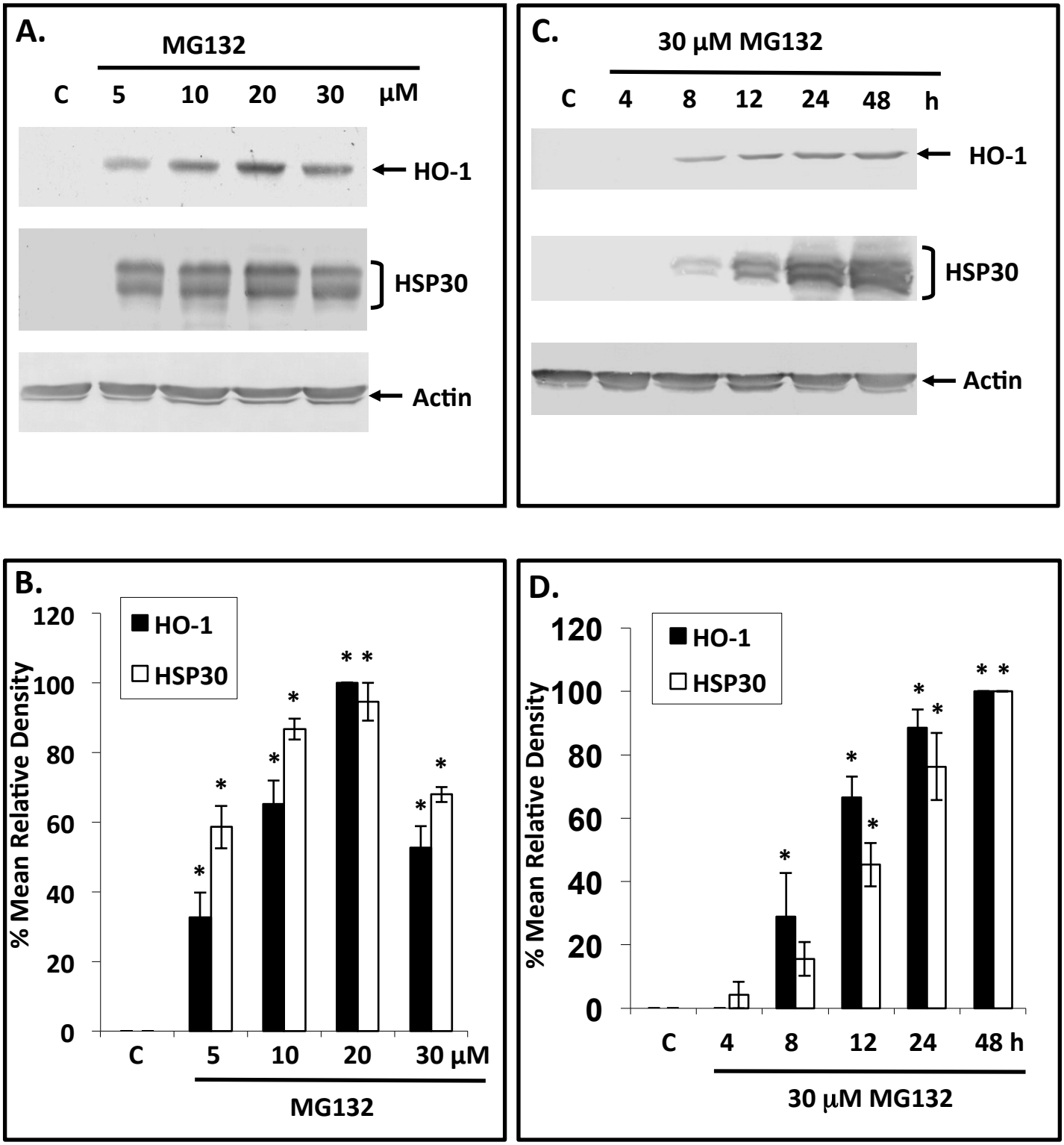
A.
MG132
C
5
10
20
30
μM
HO-1
HSP30
Actin
C.
30 μM MG132
C
4
8
12
24
48
h
HO-1
HSP30
Actin
B.
HO-1
HSP30
% Mean Relative Density
120
100
80
60
40
20
0
C
5
10
20
30 μM
MG132
D.
HO-1
HSP30
% Mean Relative Density
120
100
80
60
40
20
0
C
4
8
12
24
48 h
30 μM MG132

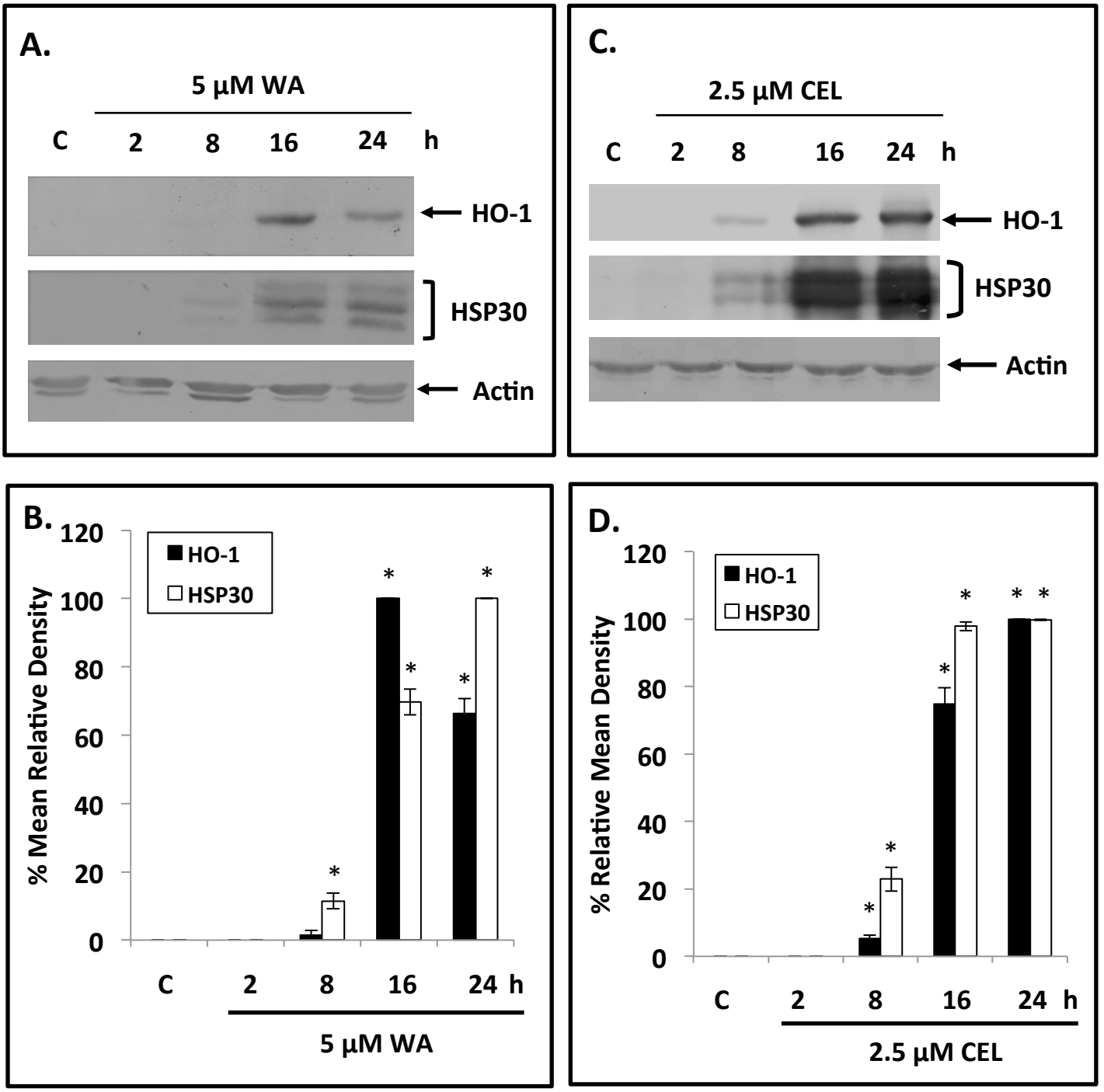
A.
5 µM WA
C
2
8
16
24
h
HO-1
HSP30
Actin
C.
2.5 µM CEL
C
2
8
16
24
h
HO-1
HSP30
Actin
B.
% Mean Relative Density
120
100
80
60
40
20
0
HO-1
HSP30
C
2
8
16
24 h
5 µM WA
D.
% Relative Mean Density
120
100
80
60
40
20
0
HO-1
HSP30
C
2
8
16
24 h
2.5 µM CEL

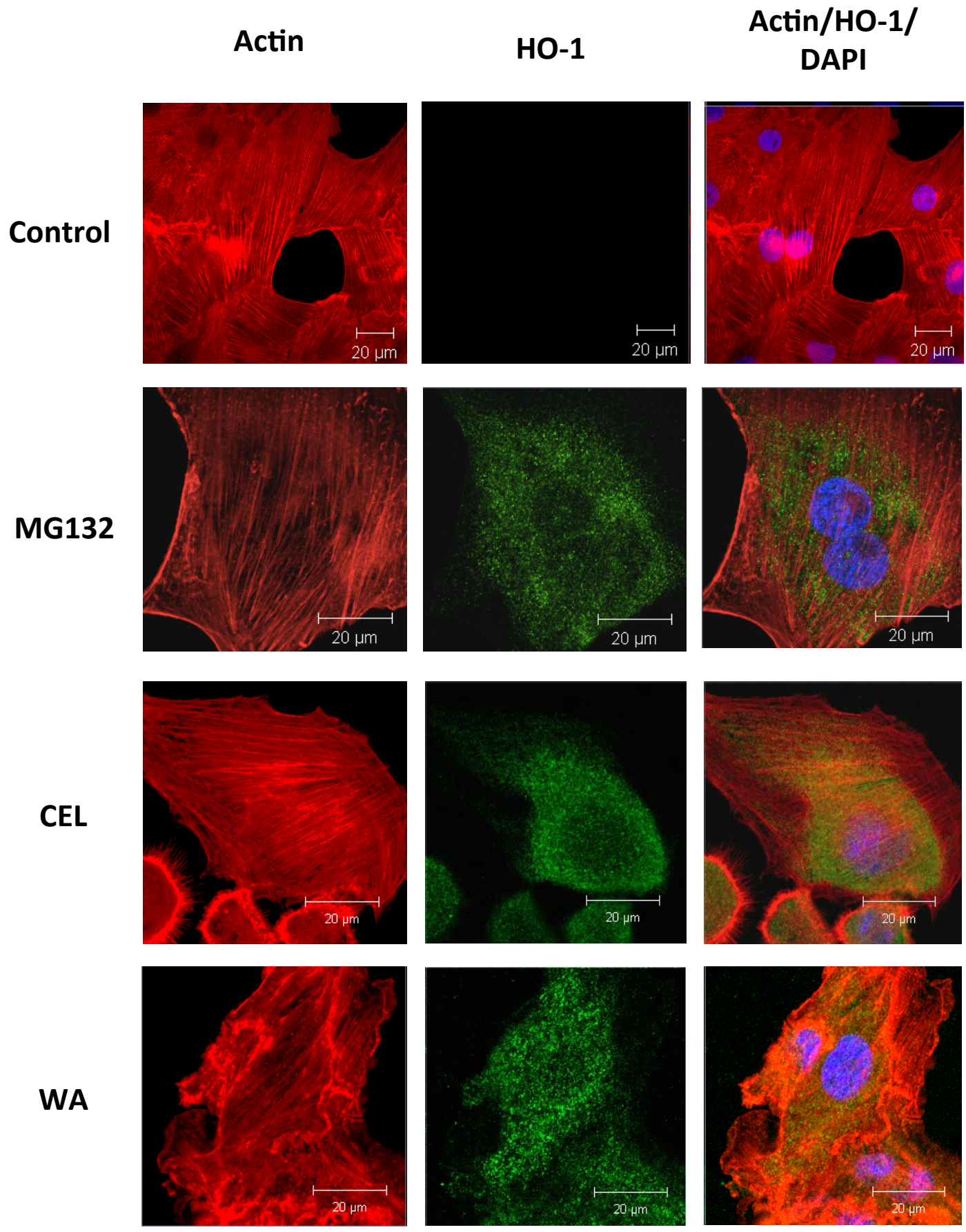
Actin
HO-1
Actin/HO-1/
DAPI
Control
MG132
CEL
WA
20 μm